REVIEW

PRECIPITATION MEASUREMENTS AND TRENDS IN THE TWENTIETH CENTURY

MARK NEW[a,*], MARTIN TODD[b], MIKE HULME[c] and PHIL JONES[d]

[a] *School of Geography and the Environment, University of Oxford, Oxford, UK*
[b] *Department of Geography, University College London, London, UK*
[c] *Tyndall Centre for Climate Change Research, School of Environmental Sciences, University of East Anglia, Norwich, UK*
[d] *Climatic Research Unit, School of Environmental Sciences, University of East Anglia, Norwich, UK*

ABSTRACT

Concern about anthropogenic climate change has heightened the need for accurate information about spatial and temporal variations in precipitation at the Earth's surface. Large-scale precipitation estimates can be derived from either surface gauge measurements or by satellite remote sensing, both of which have shortcomings. Gauge measurements provide information about trends and variability of monthly precipitation throughout the entire twentieth century, but because of the lack of data from most ocean regions, this information is representative of only about 25–30% of the Earth's surface. In contrast, satellite (especially multi-platform) measurements provide spatially complete coverage at monthly to subdaily resolution, but do not extend back beyond 1974. Merged gauge–satellite datasets maximize (and minimize) the relative benefits (and shortcomings) of each source type. While these merged products only extend back to 1979, their importance will grow as we move into the new century.

Precipitation gauge data indicate that global land precipitation (excluding Antarctica) has increased by about 9 mm over the twentieth century (a trend of 0.89 mm/decade), which is relatively small compared with interannual and multi-decadal variability. Within this century-long trend, global precipitation exhibits considerable variability on decadal time-scales, with departures of up to ± 40 mm from the century mean of about 950 mm. Regionally, precipitation has increased over most land areas, with the exception of tropical North Africa, and parts of southern Africa, Amazonia and western South America. The dominant mode of interannual variability in global and hemispheric land precipitation is related to the El Niño–Southern Oscillation (ENSO), which explains about 38% of the interannual variance in globally averaged land precipitation and about 8% of the space–time variability of global precipitation. In the mid- and high latitudes, the Arctic and Antarctic oscillation (AO and AAO) are the dominant modes of interannual climate variability. The AO explains 48 and 35% of area-averaged winter precipitation variability over land in the latitude bands 60–80°N and 40–60°N, respectively. The North Atlantic Oscillation is not an important modulator of global precipitation, but it does explain 8% of annual (more in winter) variability in spatially averaged northern mid-latitude precipitation. Analyses of precipitation over land and ocean (spatially complete) since 1980 indicate that only a few regions show marked trends in precipitation over this short period, but there is a suggestion that there has been a shift in zonal precipitation. There are coherent regions where the tropical ENSO signal extends in a northeast/southeast direction into the subtropics, especially in the Pacific-Indonesian region, but also over the Atlantic-African and Indian Ocean domains.

Data from a number of countries provide evidence of increased intensity of daily precipitation, generally manifested through increased frequency of wet days and an increased proportion of total precipitation occurring during the heaviest events. Over most land areas there has also been an increase in the persistence of wet spells. Copyright © 2001 Royal Meteorological Society.

KEY WORDS: precipitation; satellite; surface gauge; twentieth century trends; variability; climate change

* Correspondence to: School of Geography and the Environment, University of Oxford, Mansfield Road, Oxford, OX1 3TB, UK.

1. INTRODUCTION

Precipitation varies across a range of space–time scales. Larger space-scale variations generally occur at longer time scales, and are associated with correspondingly larger scale phenomena in the atmosphere or ocean–atmosphere system. For example, scales of variability within an individual convective storm may vary from metres and seconds to kilometres and hours, while the El Niño–Southern Oscillation (ENSO) related scales of variability are regional to hemispheric in extent and multi-year in length (Daly, 1991). However, these different scales are not unrelated: precipitation within individual storms is likely to be more intense and of longer duration when ENSO is causing a general enhancement in precipitation across a region. At all these time and space scales, precipitation is inherently more variable than other commonly reported climate variables, such as temperature and pressure, with the result that precipitation measurement and analysis are more demanding. Overlying this variability of precipitation within the climate system is the potential for secular changes in the intensity and distribution characteristics of precipitation.

The growing concern about climate change has heightened the need for accurate information about the space–time distribution of precipitation. At larger space scales (regional to global), precipitation data are needed for climate model evaluation (Hulme, 1994a), for the analysis of observed climate change against the background of natural variability (Hulme *et al.*, 1999a), for biogeochmeical modelling (Cramer and Fischer, 1996) and for the construction of climate scenarios for climate change impacts studies (Hulme *et al.*, 1999b). Attempts to satisfy these needs have followed two paths. Firstly, there have been numerous initiatives to collate historical precipitation gauge measurements (Hulme, 1994a; Peterson and Griffiths, 1997; Peterson and Vose, 1997; NCDC, 1998; New *et al.*, 1999, 2000; Jones *et al.*, in press), and to make existing public domain gauge data more representative and less error prone (Easterling *et al.*, 1996; Peterson *et al.*, 1997). The second route has been the development of remote sensing (predominantly satellite based) data retrieval techniques (for a review of the numerous techniques see Barrett *et al.*, 1994; Kidd, 2001). These two approaches each have advantages and disadvantages (Table I). The main advantage of gauge-based datasets is their temporal coverage, which extends back to the early decades of the twentieth century in most parts of the world, and earlier in some selected regions. The main limitation is their poor spatial coverage in many parts of the world—most notably over ocean regions, but also over land at high latitudes, in arid regions, and in parts of the tropics. In contrast, satellite-based datasets can provide spatially complete coverage, but do suffer from various discontinuities and do not extend back in time beyond the 1970s at the earliest. Recently, various 'merged' satellite and gauge analyses have gone some way to maximize (minimize) the benefits (disadvantages) of satellite and gauge precipitation measurements.

This paper reviews existing global precipitation datasets, analyses the information about precipitation trends and variability that they furnish, and highlights prospects for precipitation data provision in the future. Section 2 describes datasets derived from gauge data, including a discussion of data errors, biases and inhomogeneities, gauge coverage through time, and various interpolated gridded datasets and their associated interpolation errors and biases. Section 3 covers satellite-based precipitation datasets, including their spatial and temporal resolution, the approaches used to translate spectral information into precipitation amounts, and the error associated with such estimates. A number of efforts have been made

Table I. Some advantages and disadvantages of gauge and satellite based precipitation datasets

Gauge measurement	Satellite measurement
Poor spatial coverage	Good spatial coverage
Point measurement	Spatial measurement
Long records (maximum 350 years)	Short records (maximum 25 years)
Biases and inhomogeneities	Biases and inhomogeneities, discontinuities
Observer errors	Instrument calibration, changing algorithms

to combine gauge and satellite datasets, and these merged products are described in Section 4. In Section 5 some of the datasets described in the review are analysed to describe trends and variations in global and regional precipitation. This analysis limits itself to a discussion of what the observational record tells us about past precipitation changes. Reasons for some of the observed variations have been discussed in the Intergovernmental Panel on Climate Change (IPCC) assessments of climate change (Folland *et al*., 1990, 1992; Nicholls *et al*., 1996; Folland and Karl, 2001) and elsewhere (Chahine, 1992; Ropelewski and Halpert, 1996; Dai and Wigley, 2000). Section 6 summarizes key points from the paper, looks to the future in terms of prospects for new and/or improved datasets and data availability, and presents some conclusions.

2. SURFACE OBSERVATIONS (GAUGES)

2.1. *Precipitation measurement*

Gauges that measure precipitation at a point remain the most common approach to ground-based measurement. Although radar observations have tended to supplant gauges by providing areal estimates directly, the gauge remains the ultimate reference and is the only measurement method available in many regions of the world. Other forms of surface observation include standard present-weather classifications and more qualitative historic documentary records, such as wet day counts (Ohara and Metcalfe, 1995; Rodrigo *et al*., 1995, 1999; Kastellet *et al*., 1998; Pfister *et al*., 1999). The first rain gauge in Europe was developed by Richard Townley in Burnley, Lancashire, in 1677. Even earlier gauge measurements are believed to have occurred in Korea, where the Japanese used a type of gauge to determine the annual rice tax each region should pay. However, analyses of these data are considered unreliable as many Koreans probably understood the tax system and modified the amounts in the 'gauges' accordingly.

Gauge design (often called ombrometers in earlier times) varied considerably across Europe until some form of standardization came in the late nineteenth century (Middleton, 1953, 1965). Developments were largely dependent on climate regime, with Russian, Scandinavian and Canadian scientists emphasizing designs that maximized snow catch, particularly during strong winds. Other countries realized that catch was higher if the gauge was located at ground level rather than 1–2 m above the ground. The main result of these developments has been that nearly all long-term records of precipitation are not homogeneous, exhibiting trends and/or discontinuities attributable to design changes (see Section 2.2).

It has been estimated that at least 250 000 different precipitation gauges have been established globally by various meteorological and hydrological agencies over the last few decades (Groisman and Legates, 1995). The large majority of these were not operated for long enough to enable reliable estimates of a precipitation regime (e.g. mean and variance), where a 30-year period is often used for the calculation of climate means or 'normals' (WMO, 1996). There have been several efforts over the last few decades to collate precipitation gauge measurements into datasets with comprehensive global spatio-temporal coverage. Most of these have concentrated on monthly data, which are more readily available than daily data, particularly for earlier years. In all cases, the number of stations in the datasets increases steadily from the beginning of the century to the 1970s as more stations were established, particularly in developing countries. From the 1970s onwards, station numbers have declined, sometimes due to increasing restrictions (or costs) on the release of data by national agencies (Hulme, 1994b) and sometimes as gauge networks established for specific projects are not maintained. In other cases, the breakdown of the observing network due to economic pressure (e.g. Brazil) and/or civil unrest (e.g. Sudan) has also contributed to the decrease in data.

Probably the most comprehensive dataset for the years after 1985 resides with the Global Precipitation Climatology Centre (GPCC), which is a part of the World Climate Research Program. The GPCC processes monthly and daily data from the Global Telecommunication System (GTS), as well as from over 140 different meteorological and hydrological organizations around the world. There was a maximum of about 38 000 active stations in the database in 1988, but these have declined steadily to a

core of the 7000 GTS stations by the end of 1999 (Rudolf, personal communication). Unfortunately, these station data are not in the public domain because of the bilateral agreements reached between the GPCC and contributing organizations. The GPCC gridded precipitation datasets (1.0° × 1.0° resolution) derived from the station data are, however, in the public domain (see Section 2.3).

The most comprehensive dataset of monthly precipitation covering the entire twentieth century is the Global Historical Climatology Network (GHCN). The GHCN represents a major co-operative effort, with many organizations and individuals having contributed data. This dataset comprises some 31 000 stations with varying temporal coverage. Some stations provide records over 100 years in length; others last for only a few years. The maximum number of stations contributing to GHCN in any one year is just under 16 500, in 1966 (Figure 1). This contrasts with 5500 in 1900 and 8000 in 1996. Station numbers decrease to 2500 by the year 2000, but are likely to increase with time as data not available over the GTS 'filter' through to the GHCN (e.g. via the decadal publications of the World Meteorological Organization (WMO)). These large station numbers also mask regional disparities, with tropical regions and high latitudes being poorly represented, particularly before 1950 (Figure 2).

The Global Summary of the Day (GSD) dataset of daily precipitation represents an effort by the NOAA to make use of synoptic data available over the GTS. This dataset is of relatively short duration (1977–1991) and is error prone (e.g. Piper and Stewart, 1996) and is not covered further in this review, which concentrates on monthly data.

2.2. Data errors

Precipitation data are subject to errors, biases and inhomogeneities arising from several sources. Inaccurate measurements for individual days and months most often arise through observer errors, either during measurement or transcription to paper or digital records. Detection of such errors is particularly difficult because the skewed distribution of daily (and to a lesser extent monthly) precipitation amounts implies that in all but the most extreme cases a suspect measurement has a considerable likelihood of being real. Comprehensive checking of suspect measurements is time consuming, usually requiring comparison with nearby station data, station metadata, documentary records and possibly, original registers. Such an approach is impossible to apply comprehensively when dealing with global datasets and various automated procedures have been used. These are usually based on the identification of data points
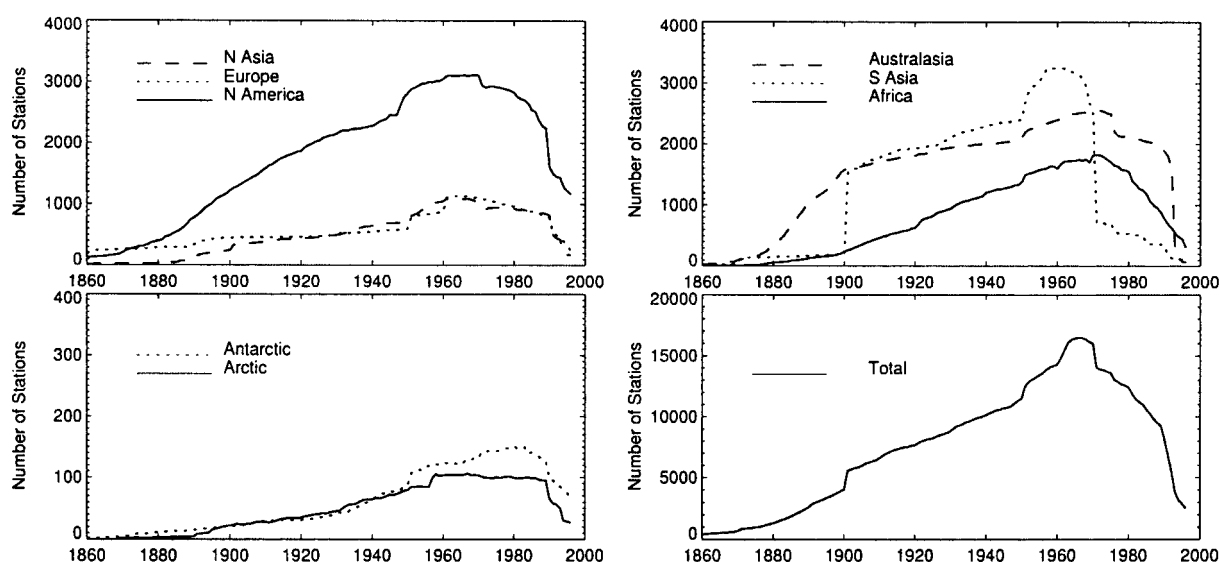

Figure 1. Global and regional station numbers in the GHCN from 1850 to present
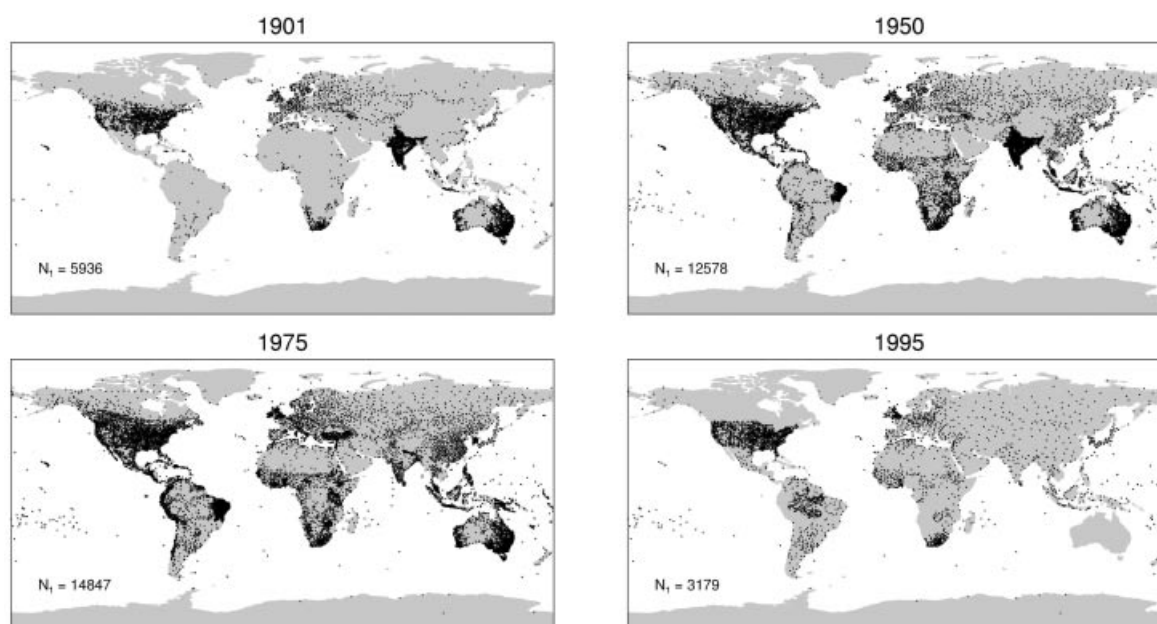
Figure 2. Space–time distribution of the GHCN precipitation station dataset

outside a predefined confidence interval for a standard statistical distribution (usually either normal, power of normal or gamma) and on the identification of discontinuities in time series (e.g. Easterling and Peterson, 1995).

Measurement biases arise because of gauge undercatch (UNESCO, 1978; Sevruk, 1982; Groisman *et al.*, 1991; Legates and DeLiberty, 1993; Peterson *et al.*, 1998) caused mainly by turbulence around the gauge deflecting precipitation, but also by other factors such as raindrops splashing out of the gauge and evaporation. Undercatch is most severe for snowfall, where amounts can be underestimated by up to 50%, depending on gauge design, site exposure, wind conditions and snow character. Legates and Willmott (1990) derived mean monthly correction factors for gauge undercatch as a function of several parameters, and estimated a global mean undercatch of precipitation of about 11%. This global estimate masks strong latitudinal gradients (primarily due to the relative frequency of snowfall) and temporal variations at any particular gauge. Estimates of gauge undercatch relating to snowfall are further complicated by trends and variability in temperature; warmer (colder) winters are associated with less (more) solid precipitation, and therefore less (more) undercatch. Various authors have either corrected for gauge biases (e.g. Rudolf *et al.*, 1994; Yang, 1999; Yang *et al.*, 1999) using generalized formulas, such as those of Legates and Willmott (1990), or ignored them (e.g. New *et al.*, 2000), acknowledging that they affect the resulting dataset.

A homogeneous climate record is defined as one where the only variations in the record are due to climate. Inhomogeneities in station precipitation series occur because of changes in gauge type, observing practices, location or site conditions (Peterson *et al.*, 1998). In the strictest sense, a precipitation record can only be considered homogeneous over a few months or years because of changing site conditions (vegetation, buildings, etc.). Gradual site changes, which produce slow changes in the precipitation record, are difficult to detect and are generally ignored. More pronounced site changes, along with changes in gauge type and locations usually result in a 'jump' or step in the record and are easier to detect. Automated and manual methods for the detection and correction of trends and inhomogeneities are reviewed by Peterson *et al.* (1998).

The seriousness of different types of errors and inhomogeneities in precipitation records depends on the spatial scale of analysis and the spatial extent of any inhomogeneity. For analysis of climate change and

trends at regional and larger scales, the effects of errors and inhomogeneities at individual stations are reduced in the averaging of multiple station series that occurs in the calculation of regional time series (New, 1999). Inhomogeneities may also be regional in extent, for example, where observer practices are changed, or widespread changes in gauge type occur in a country (Groisman *et al.*, 1991; Heino, 1994). Where such region-wide changes occur regional trends will also be affected, though the analyses of Dai *et al.* (1997) indicate that it is only over the former USSR that a regional inhomogeneity due to instrument effects occurs (a non-climatic increase in recorded precipitation of about 40% from the 1940s to the early 1950s). Moreover, for a country such as the former USSR, the problem is to a large extent correctable (Groisman and Rankova, 2001).

2.3. Gridded precipitation datasets

Gridded precipitation datasets are required for a range of climatic and related applications (see Section 1). For the analysis of regional precipitation trends, gridding is a necessary preliminary step that helps to reduce biases arising from the irregular station distribution shown in Figure 2 (Jones and Hulme, 1996; Dai *et al.*, 1997). Several gridded datasets of monthly precipitation or precipitation anomalies (relative to some long-term mean) have been developed in recent years (summarized in Table II). There have been two broad approaches to interpolation of station data to produce gridded datasets, each arising due to different applications.

In the first approach the resultant grids have primarily been used for analysis of twentieth century precipitation trends and variability. Precipitation is only estimated at grid cells containing precipitation station data (Hulme, 1994a, updated; henceforth HULME) or at grid cells at which there is at least one contributing precipitation station within an empirically defined distance from the grid cell centre (Dai *et al.*, 1997; henceforth DAI). In this respect, the DAI gridding procedure makes use of a more generous 'search radius' in selecting stations to be included in estimating a grid point value, but greater weight is assigned to stations closer to the grid centre through an inverse-distance weighting scheme. A consequence of both these approaches is that the number of grid cells at which estimates are calculated varies spatially and temporally as contributing stations fall in and out of the dataset.

In the second approach, the emphasis of the gridding exercise is to produce precipitation fields that are continuous in space and time over land areas. Such grids are typically used as input for global and regional grid-based simulation models, such as terrestrial biogeochemical models. In data-sparse regions, precipitation estimates make use of more distant stations, and the associated interpolation error increases. Three widely available monthly precipitation datasets have been constructed using variants of this approach: the GPCP 1° by 1° and 2.5° by 2.5° latitude/longitude datasets, extending from 1986 to within a few months of the present (Rudolf *et al.*, 1994); the Xie *et al.* (1996; henceforth

Table II. Datasets of global precipitation gauge data

Name	Network size	Time step	Time period	Reference
GHCN[a]	Up to 31 000	Monthly	1800s–present	Peterson and Vose, 1997
GPCP/GPCC[b]	Up to 38 000	Monthly	1986–present	Rudolf *et al.*, 1999
CRU[c]	Up to 15 000	Monthly	1700s–present	Hulme, 1994a; New *et al.*, 2000
MCDW[d]	Up to 2000	Monthly	1961–present	NCDC[f] on behalf of WMO
GSD[e]	Up to 10 000	Daily	1977–1991	

[a] Global Historical Climatology Network.
[b] Global Precipitation Climatology Project/Centre.
[c] Climatic Research Unit.
[d] Monthly Climatic Data for the World.
[e] Global Summary of the Day.
[f] National Climate Data Center.

XIE) 2.5° latitude/longitude dataset, which uses additional data from earlier years to extend the GPCP product back to 1971 (note that this is not an official GPCP product and that a new version extending the temporal coverage back to 1950 is under development—Xie, personal communication, 2001); and the Climatic Research Unit 0.5° by 0.5° latitude/longitude dataset, extending from 1901 to 1999 (but updated on an annual basis; New et al., 2000; henceforth NEW).

All the above gridded datasets except HULME employ a variant of Shepard's (1968,1984) inverse distance weighting scheme, altered to incorporate spherical co-ordinates after Willmott et al. (1985). They simply differ in the number of stations that are used for each estimate and the formulation of the distance weighting function. The HULME dataset uses Thiessen's (1911) weighting, in which stations are assigned weights according to the area of the grid-box they represent, and not their distance from the grid-box centre; however, missing data from stations in the selected Thiessen network are first estimated using Shepard's scheme. There are also other subtle differences in the interpolation methods. NEW and DAI estimate precipitation at grid-box centres, so their estimates tend towards being point values (stations nearer the grid centre receive greater weight). GPCP and XIE first estimate precipitation at the centres of 0.5° grid-boxes, and subsequently estimate the area-mean precipitation at each 2.5° (1°) latitude/longitude box by taking the area-weighted average of the 25 (4) 0.5° estimates inside it; as a result their estimates tend towards being areally averaged values. The Thiessen averaging employed in HULME also generates area-averaged estimates.

A final difference between the datasets concerns whether the station data are transformed in any way prior to interpolation. GPCP and XIE simply interpolate station precipitation depths, which can present problems if interpolating over data-sparse areas with steep gradients in mean precipitation. DAI and NEW first transform station data into anomalies relative to a standard normal period prior to interpolation. The interpolated anomaly fields are then back-converted to precipitation depths by combination with a precipitation climatology for the normal period. The advantage of the 'anomaly' approach is that the number of archived and easily obtainable station normals is far greater than that of station time series, particularly as one goes back in time (New et al., 1999, 2000). Using as many stations as possible to generate a mean precipitation climatology maximizes the representation of spatial variability in mean climate. Monthly anomalies, on the other hand, tend to be more a function of large-scale circulation and a comparatively less extensive network may be sufficient to describe the month-to-month departures from the mean climate. In converting to anomalies, DAI express their anomalies in mm units, while NEW, in an attempt to preserve some of the dependence of precipitation variance on mean precipitation, express anomalies as percentages of the mean.

These varying interpolation schemes inevitably lead to different estimates of monthly precipitation depth and the variability. While there is considerable overlap in the stations contained in the input datasets (Section 2.1), the main cause of differences between the gridded analyses is undoubtedly due to differing station networks, particularly in data-sparse regions, where only one or a few independent gauge measurements may contribute to each dataset. For example, Xie et al. (1996) when comparing XIE and GPCP found mean absolute differences (MAD) of around 15% at grid cells with five or more stations within a 2.5° box in both datasets; the MAD increased to 40–90% in grid cells where both datasets had only one station within a 2.5° box. These MAD are similar to sampling errors in precipitation anomalies at 2.5° latitude/longitude resolution estimated theoretically by Dai et al. (1997): they report relative errors to be ~14% and ~45% for grid boxes containing five and one stations, respectively. Our own analysis, comparing HULME and DAI over the period 1951–1991, shows similar mean differences (not shown). Xie et al. (1996) also showed empirically that estimation errors arising from interpolation of precipitation depth tend to be biased towards overestimation of large precipitation amounts and underestimation of smaller precipitation amounts. Whether this bias also occurs during interpolation of transformed data (i.e. anomalies) has not been investigated.

3. SATELLITE OBSERVATIONS

Precipitation estimates over large areas are often most easily obtained from satellite data. Indeed, satellite data provide the only means of obtaining quantitative information on precipitation over much of the oceans, where the majority of the world's rain falls, and for many inaccessible land regions. For this reason, attempts to derive estimates of precipitation from satellite data have a long history dating from the early 1970s.

3.1. Approaches to satellite estimation of precipitation

A remote sensing method can be either passive or active. Passive methods rely on natural thermal emission of electromagnetic radiation (EMR) from rain clouds or on solar radiation reflected from them. Active sensors generate the radiation and record its reflection from targets in the atmosphere. However, satellite-borne active microwave systems, such as the Tropical Rainfall Monitoring Mission (TRMM) Precipitation Radar (Kummerow *et al.*, 1998) are a relatively recent development and have produced only a very short record commencing in late 1997. On the basis of our understanding of the complex interaction of EMR with the Earth's surface and the intervening atmosphere, consisting of clouds, water vapour and liquid and frozen precipitation, it is possible to derive quantitative information on rain intensities at the time of the satellite observation. For a full review of satellite precipitation algorithms see Kidd (2001). Here the aim is to provide an overview of satellite methods that contribute to long-term precipitation datasets. A brief summary of the characteristics of a selection of principal precipitation products derived from satellites is provided in Table III.

The earliest meteorological satellites carried sensors that recorded in the visible (VIS) and thermal infrared (IR) portions of the EMR spectrum, and it is for this type of data that we have the longest available record. Thermal IR emission occurs 24 h a day, so this data type has proved more useful in itself than the VIS observations. In deriving quantitative estimates of precipitation from IR data it is generally assumed that high clouds (with cold tops) are most likely to precipitate. This assumption is sustained most often in convective precipitation systems, in which the amount of cold cloud is related to the amount of vertical uplift. Accordingly, these methods are often restricted to the tropics and wet season subtropics (30°N–30°S), rather than in the mid-latitudes, where baroclinic systems dominate. Methods based on IR data can mostly be described as cloud-indexing methods, whereby the coverage of cloud with cold tops over some space and/or time domain is related to surface precipitation through an empirically derived relationship. An example of this is the GOES Precipitation Index (GPI) of Arkin and Meisner (1987). Such methods are most accurate when the space/time domain is large (e.g. 2.5° by 2.5° by 12 h) providing a sample that is representative of meteorological 'average' conditions.

Errors and biases result from space/time variations in the relationship between cold cloud cover and precipitation. There are indications that the GPI may overestimate (underestimate) deep (shallow) convective precipitation over land (ocean) areas (Petty, 1997). Successful modifications of the GPI have recently emerged in which the IR threshold and rain rate are calibrated locally using information on precipitation from gauge data (Todd *et al.*, 1995, 1999) or microwave satellite data (Hsu *et al.*, 1999; Todd *et al.*, 2001). Nevertheless, the GPI and the reconstructed GPI (Todd and Washington, 1999) provide one of the most extensive quantitative records of precipitation available for the global tropics and subtropics on a 2.5° grid from 1986 to present, at resolutions ranging from monthly to 3 hourly, in the case of the RGPI.

Satellite estimates of outgoing longwave radiation (OLR) flux have been widely used as a surrogate for convective precipitation, at least in the tropics. The method of Gruber and Krueger (1984) converts narrow band IR measurements from NOAA satellites into broadband estimates of OLR using a radiative transfer model. This dataset now extends from mid-1974 to present and has supported numerous climate studies. Precipitation estimates can be derived from OLR using the method of Wu (1991), which through inclusion of differences in clear sky minus cloudy sky OLR and diurnal contrasts in clear sky OLR is sensitive to both the radiative effect of rain cloud and its effect on soil moisture.

Table III. Characteristics of selected satellite and merged global precipitation datasets

Product name	Data source	Coverage		Resolution		Reference
		Spatial	Temporal	Spatial	Temporal	
GPI[a]	Geostationary IR	40°N–40°S	1986–present	2.5°	Pentad and monthly	Arkin and Meisner (1987)
Reconstructed GPI	ISCCP D1 and IR[b]	40°N–40°S	1986–present[c]	2.5°	3 hourly	Todd and Washington (1999)
NOAA/ NESDIS/ ORA	DMSP SSM/I	60°N–60°S	1987–present[d]	1.0° and 2.5°	Monthly	Ferraro et al. (1996)
GPROF 4.0[e]	DMSP SSM/I	90°N–90°S	1987–present	0.5°	Instantaneous	Kummerow and Giglio (1994a,b)
MSU[f]	NOAA MSU	60°N–60°S[g]	1979–present	2.5°	Monthly	Spencer (1993)
GPCP 1-degree daily	GPI, SSM/I (GPROF), GPCP gauge, TOVS	90°N–90°S	1996–present	1.0°	Daily	Huffman et al. (2000)
NOAA CMAP	GPI, SSM/I, GPCP gauges, NWP[h]	90°N–90°S	1979–present	2.5°	Pentad and monthly	Xie and Arkin (1996)
GPCP monthly merged	GPI, SSM/I, GPCP gauges	90°N–90°S	1987–present	2.5°	Monthly	Huffman et al. (1997)
CRU	OLR, gauges (HULME)	30°N–30°S	1974–1994	2.5 * 3.75°	Monthly	Doherty et al. (1999)

[a] GOES Precipitation Index.
[b] Geostationary and polar orbiting IR.
[c] At time of press not all ISCCP D1 data for the period 1986–present was available.
[d] With gaps from 7/90 to 12/91.
[e] Full name: GPROF 4.0 Gridded Orbit-by-Orbit Precipitation Data Set.
[f] Microwave Sounding Unit.
[g] Oceans only.
[h] Numerical Weather Predictions.

In the extratropics, IR algorithms are much less successful. However, despite the inherent problems of IR data, Susskind *et al.* (1997) describe a method that derives precipitation from cloud parameters retrieved from the TIROS Operational Vertical Sounder (TOVS) instrument. The algorithm is based on empirically derived regression relationships stratified by latitude, season and surface type.

In contrast to thermal IR or VIS EMR, microwaves (particularly the longest wavelengths) can penetrate into cloud regions such that they interact more directly with ice or liquid hydrometeors, often providing more accurate estimates of rain rate. Numerous algorithms have been developed over the years since the launch of microwave instruments (notably the Microwave Sounding Unit in 1979 and Special Sensor Microwave Imager in 1987). These can be categorized as either empirical or physically based. In the former case a simple index of observed microwave brightness temperatures (often multi-frequency or polarization) is related to precipitation through an empirically derived relationship. The NOAA algorithm (Ferraro *et al.*, 1996) is perhaps the most widely used. Physically based algorithms utilize a radiative transfer model for variational optimization in which cloud and precipitation profiles are varied until an optimal match with observed MW brightness temperatures is achieved. The Goddard Profiling (GPROF) algorithm (Kummerow and Giglio, 1994a,b) is perhaps the most widely used example of this. The MSU provides the longest continuous record from a single MW sensor type from which precipitation estimates can be derived, although only over oceans (Spencer, 1993). While MW algorithms can provide much more accurate estimates of instantaneous rain rate, they suffer from a range of errors and biases. Of particular note is the sampling bias of sensors on sun-synchronous satellites. Bell and Kundu (2000) provide a review of this issue.

Validating satellite precipitation estimates has been a major focus in recent years with numerous intercomparison projects undertaken at regional (WCRP Algorithm Intercomparison Projects) and global (NASA WetNet Precipitation Intercomparison Projects) scales. Summaries of the results of AIP 1–3 can be found in Ebert *et al.* (1996) and Ebert and Manton (1998) and of PIP-1 and PIP-2 in Barrett *et al.* (1994) and Smith *et al.* (1998), respectively. Although the findings are too numerous to summarize here, a number of important points emerge. First, no single-satellite algorithm performs best in all conditions over all surfaces. Second, accuracy of satellite methods is dependent on location and time. Third, MW methods produce more accurate estimates of instantaneous rain rate compared with IR. Fourth, the source of variability between MW algorithm estimates differs for land and ocean algorithms (Smith *et al.*, 1998). Finally, algorithms that involve gauge calibration generally perform better than satellite-only techniques.

To provide a quantitative overview of algorithm performance the results of the most extensive validation conducted to date (PIP-3) are instructive. A number of satellite algorithms were evaluated by comparison of monthly precipitation estimates at 2.5° resolution over a 12-month period (January–December 1992) with those from rain gauge data (from the GPCC dataset) at 216 land grid cells and 15 tropical Pacific cells centred on atolls (indicative of oceanic conditions). Here, we summarize the results from those algorithms that are fully independent of gauge data. Over land, using 14 satellite algorithms, the mean (standard deviation; SD) ratio of satellite to gauge monthly precipitation was 0.94 (0.19), while the mean (SD) of root-mean-squared errors (RMSE, mm/month) was 63.4 (8.0). A total of 21 algorithms were compared with atoll rain gauge data and the mean (SD) ratio of monthly precipitation was 0.79 (0.2) and RMSE was 127.3 (20.0). The mean RMSEs were 78% and 55% of the mean gauge estimates over land and ocean, respectively, providing a clear idea of the magnitude of errors (relative to gridded gauge products) associated with satellite estimates of monthly precipitation. The 'best' satellite algorithms produced RMSEs of 67% of the mean gauge estimate over land (using an 'optimal' combination of numerous satellite algorithms) and 41% over oceans (using GPI). However, it is important to note that all the validation statistics include errors in the gauge as well as satellite quantities.

Results from the validation of numerical weather prediction model reanalysis datasets against gauge data were comparable, such that while the better satellite algorithms provide useful improvements, on average the satellite performance is similar to models. However, the relative accuracy of satellite estimates may well be higher in more remote regions where model initialization data are more limited. Validation statistics for merged products (see Section 4) were greatly superior to all other products, but comparison

is problematic since the validation data are not independent of the merged product. Nevertheless, given that merged products involve an 'optimized' combination of a number of algorithms it is highly likely that they represent our most accurate estimates of truly global precipitation.

4. COMBINED DATASETS

The shortcomings of single-satellite (or surface-based) data types have stimulated the development of merged precipitation products. To satisfy the requirement from the climate community for spatial fields of accurate estimates of global precipitation, the WCRP established the Global Precipitation Climatology Project (GPCP). The resulting GPCP combined precipitation dataset provides monthly estimates on a 2.5° grid from 1986 to present. The method (Huffman *et al.*, 1997) involves a sequential merging of input estimates from satellite MW, IR and rain gauge observations. The gauge dataset used is that produced by the GPCC (see Section 2.3). At each stage biases are removed where possible. For example, over land grid cells the satellite estimate is scaled by the ratio of the gauge and satellite estimates over a larger 5° × 5° grid cell window to produce a satellite–gauge quantity. Crucial to the method is an estimate of the random error of each estimate input at each grid cell, largely a function of the estimated mean rain rate and the number of samples. The merging procedure weights the individual input components by the inverse of the random error to produce a final merged product. An experimental version includes estimates from Numerical Weather Prediction models in regions (e.g. the polar oceans) where other data are unavailable.

The Climate Prediction Centre Merged Analysis of Precipitation (CMAP) product of Xie and Arkin (1996) provides precipitation estimates at the same space and time scales (although covering a longer period from 1979 to present) and uses a similar set of input data (satellite MW, IR (GPI), GPCC rain gauge including ECMWF NWP analyses) and a similar, though more complex, merging technique. In this case, though, the method has two steps: (i) reduce the random error and (ii) reduce the bias of the estimate. In (i) a 'combined' estimate is derived from the four satellites and NWP products, which are merged by a maximum likelihood procedure where, like the GPCP product, the weighting factors are the inverse of the individual random error. The random errors are defined for land areas by comparison with the gauge data and over ocean by comparison to atoll gauge data where available and by subjective extrapolation elsewhere. In the second step (ii) the final blended estimate is derived using an iterative procedure that maintains the relative distribution of the combined estimate and the amplitude of the GPCC gauge estimate. In both the GPCP and CMAP products it is assumed that the bias of the gridded gauge product is minimal, which as we have seen (Section 2.3) is not always the case.

Recently, truly global daily precipitation estimates (since 1996) on a 1° grid resolution have been produced by merging of GPI (calibrated locally using the MW GPROF algorithm) within the latitude band 40°N–40°S with TOVS precipitation estimates over the extra tropics (Huffman *et al.*, 2000). The procedure involves scaling the daily estimates such that the monthly total matches those of the monthly GPCP product described above. The product uses IR data archived for this purpose under the auspices of WCRP GEWEX. A similar combined MW/IR technique (MIRA), when applied to ISCCP DX satellite IR data, provides the potential for estimates of precipitation at 30 km/3 hourly resolution from 1986 to present, at least over the global tropics and subtropics (Todd *et al.*, 2001). The method of Doherty *et al.* (1999) combines OLR and HULME rain gauge data to provide monthly estimates of precipitation from 30°N to 30°S on a 2.5° × 3.75° grid.

5. TRENDS AND VARIABILITY

Precipitation data derived from gauge and satellite/merged sources provide contrasting opportunities for the analysis of precipitation variability in space and time. From the perspective of climate change, it is only gauge data that provide the century-long temporal coverage suitable for the identification of secular
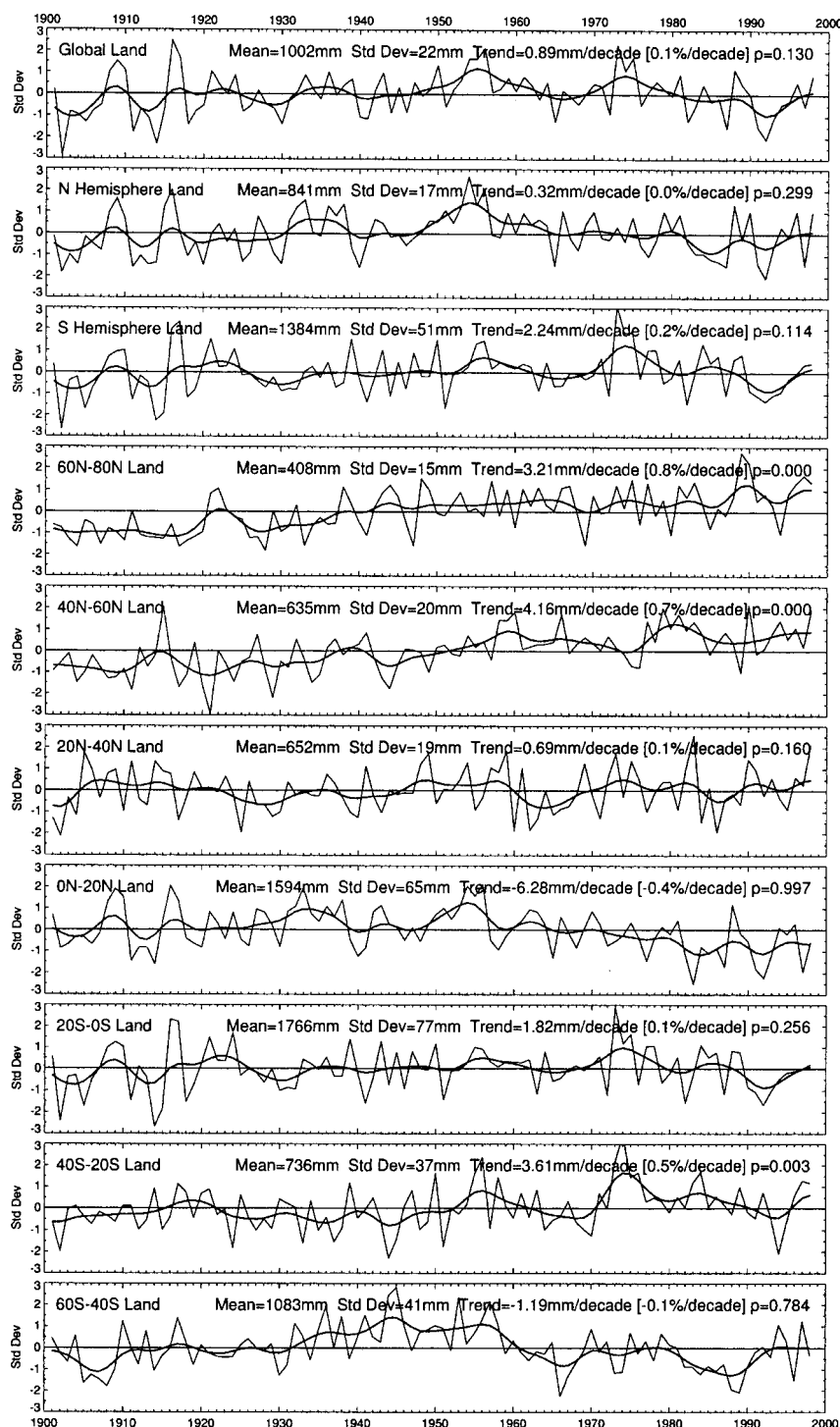
Figure 3. Area-averaged precipitation trends for various domains over the globe, calculated using the NEW dataset. Domain means, standard deviations and linear trends (all for the period 1901–1998) are also shown. p values represent the probability that such a trend could have arisen from a random normally distributed dataset with the same standard deviation as the observed series (essentially a signal-to-noise measure)

trends. In doing so, however, the oceanic areas are largely ignored (apart from precipitation over ocean islands). This is a limitation because the greater proportion (70%) of global precipitation occurs over the ocean, although the areas of the Earth that are important for human and terrestrial resources are adequately represented by gauge datasets.

5.1. Twentieth century trends over land areas

Area-averaged regional precipitation anomalies for global, hemispheric and 20°-zonal land domains are shown in Figure 3 and the spatial pattern of trends are shown in Plate 1. These zonal series were derived from the 0.5° latitude/longitude dataset of global land precipitation described by New *et al.* (2000), using a weighting scheme to account for latitudinal changes in grid-cell area. The results agree with earlier analyses (Bradley *et al.*, 1987; Diaz *et al.*, 1989; Dai *et al.*, 1997), with global precipitation having an increasing trend of 0.89 mm/decade. Within this century-long 'stability', however, global land precipitation gradually increased by about 40 mm from 1901 to the mid-1950s, remained above the century-long mean until the 1970s and then declined by about the same amount to 1992. Since 1992 global precipitation has recovered towards the century mean. The magnitude of the century-long trend of ~ 9 mm is quite small compared with this multi-decadal (and also interannual) variability. The peak in global precipitation between 1950 and 1960 has been shown by Dai *et al.* (1997) to be real and not an artefact of changing station networks. These authors also reported a secular increasing trend in global precipitation of 2.4 mm/decade when North Africa was excluded from their analysis (they argued that the post-1950s decline in precipitation over North Africa should be excluded from an analysis for secular trends because it represents a multi-decadal oscillation rather than a secular change). If the North African domain is excluded from our analysis, a positive trend of 1.8 mm/decade results, which is in close agreement with Dai *et al.* Finally, if the analysis is repeated for the period 1901–1988 (the same period as Dai *et al.*) then the resulting trend in global land precipitation is 2.48 mm/decade, essentially the same at that reported by these authors. Thus, the addition of 10 years of data in the 1990s, with below-average global precipitation, has reduced the estimated century-long trend by about 25%.

As might be expected, precipitation in both Southern and Northern Hemispheres is highly correlated with the global signature (Table IV) but they are not well correlated with each other. Global and hemispheric precipitation are closely correlated with precipitation in the tropics because these are regions with highest precipitation and relatively high latitudinal weighting (i.e. the relative area per land cell is highest in the tropics). These two factors combine to outweigh the effect of the greater number of land cells occurring at mid to high northern latitudes. This effect is even larger for Southern Hemisphere precipitation, where the hemispheric signal is dominated by the precipitation between 0° and 20°S.

Relatively large positive trends of 4.16 and 3.21 mm/decade occur in the Northern Hemisphere mid-latitudes (40°–60°N) and high latitudes (60°–80°N), reflecting the increasing linear trends over almost all land areas in these zones (Plate 1). These trends may be partly gauge related, particularly over the former Soviet Union, where the introduction around 1950 of the Tretyakov gauge—which measures

Table IV. Correlations between annual precipitation from global, hemispheric and zonal domains

	Global	NH	SH	60–80°N	40–60°N	20–40°N	0–20°N	0–20°S	20–40°S	40–60°S
Global	1.00	0.74	0.85	0.22	0.02	0.07	0.70	0.86	0.30	0.08
NH		1.00	0.28	0.17	0.23	0.26	0.84	0.32	−0.07	0.14
SH			1.00	0.18	−0.14	−0.10	0.35	0.97	0.49	0.01
60°–80°N				1.00	0.22	0.18	−0.12	0.15	0.18	−0.02
40°–60°N					1.00	0.14	−0.19	−0.17	0.08	−0.10
20°–40°N						1.00	−0.14	−0.12	0.04	−0.04
0°–20°N							1.00	0.41	−0.15	0.19
0°–20°S								1.00	0.28	0.01
20°–40°S									1.00	−0.21
40°–60°S										1.00

snowfall more accurately—increased recorded winter precipitation by up to 40% (Groisman *et al.*, 1991; Dai *et al.*, 1997; Groisman and Rankova, 2001). Nonetheless, the trends agree with those calculated by Dai *et al.* (1997), who adjusted their records for discontinuities and showed that most of the high latitude increases occurred in spring. This increase is likely to be at least partly due to warming in these high latitudes producing more liquid precipitation in spring (and hence more efficient gauge catch).

Precipitation in the northern subtropics (20°–40°N) does not have a trend through the twentieth century and is characterized by subdecadal variability. In contrast, the northern tropics (0°–20°N) exhibit a marked decrease of 6.3 mm/decade, most of which has occurred since the mid-1950s; prior to this precipitation remained close to or above the century mean. The post-1950s drying is largely a reflection of the decrease in precipitation over tropical North Africa, associated with the well-documented Sahelian drought. In the Southern Hemisphere, the tropics (0°–20°S) have remained roughly constant on a century time scale. However, the subtropics (20°–40°S) exhibit an increasing trend of 3.6 mm/decade. Between 40° and 60°S there is no marked trend, but land precipitation was below average until 1930, above average from 1930 to 1960 and then below average until the last few years. It should, however, be noted that this domain is represented only by southern South America and New Zealand, and therefore has a relatively small land area.

5.2. Secular trends over oceanic regions

The absence of spatially extensive long-term observations over the oceans makes the identification of secular trends over these regions difficult. The trends over tropical oceanic islands (Plate 1) suggest that large parts of the oceans have coherent trends, with most of the tropical eastern Pacific islands exhibiting increasing trends and the western Pacific islands having decreasing trends. These trends are likely to be related to the increased frequency and/or intensity of ENSO events in the second half of the twentieth century. Over the Indian Ocean, most western islands exhibit a slight drying, while the few islands present in the east show a slight increasing trend. Data from the Atlantic Ocean are sparse, but there is a suggestion of increasing (decreasing) precipitation in the southern (northern) tropical Atlantic.

Figure 4 shows area-averaged trends in precipitation from islands in the three tropical oceans and global tropical oceans. If these series are taken as proxies for the gross behaviour of precipitation in the tropical oceans (which will be the dominant factor in the global oceanic signature), there is evidence of an overall decrease in tropical ocean precipitation (6.4 mm or ∼ 0.3% per decade). These changes are made up of decreases in the western Pacific, Atlantic and Indian basins, and increases in the eastern Pacific basin.

5.3. Recent trends and variability over land and ocean

Although the absence of long-term observations over the oceans precludes the rigorous identification of secular trends, satellite observations and combined datasets provide a record of land–ocean precipitation since the late 1970s. There is still a substantial debate over the estimation of the mean climatological precipitation from various methods, highlighted by the results of international intercomparison projects such as NASA's WetNet PIP-1 and PIP-3 (Barrett *et al.*, 1994). However, estimates of precipitation from satellite have enabled studies of precipitation variability at decadal, interannual and intraseasonal time scales. In this context, application of satellite data to trend detection must be conducted with the utmost caution as satellite datasets suffer from several limitations:

 (i) The brevity of the satellite record relative to surface gauge data, such that trends are sensitive to the effects of interannual variability.
 (ii) The lack of a single truly global algorithm applicable over all surface types.
(iii) Errors associated with individual satellite sensors.
(iv) Systematic bias associated with changes in satellites within the record. Most meteorological satellites have a lifespan of a few years such that numerous satellite instruments contribute to the longer-term records. Biases can arise from both instrument calibration characteristics and equatorial crossing times.
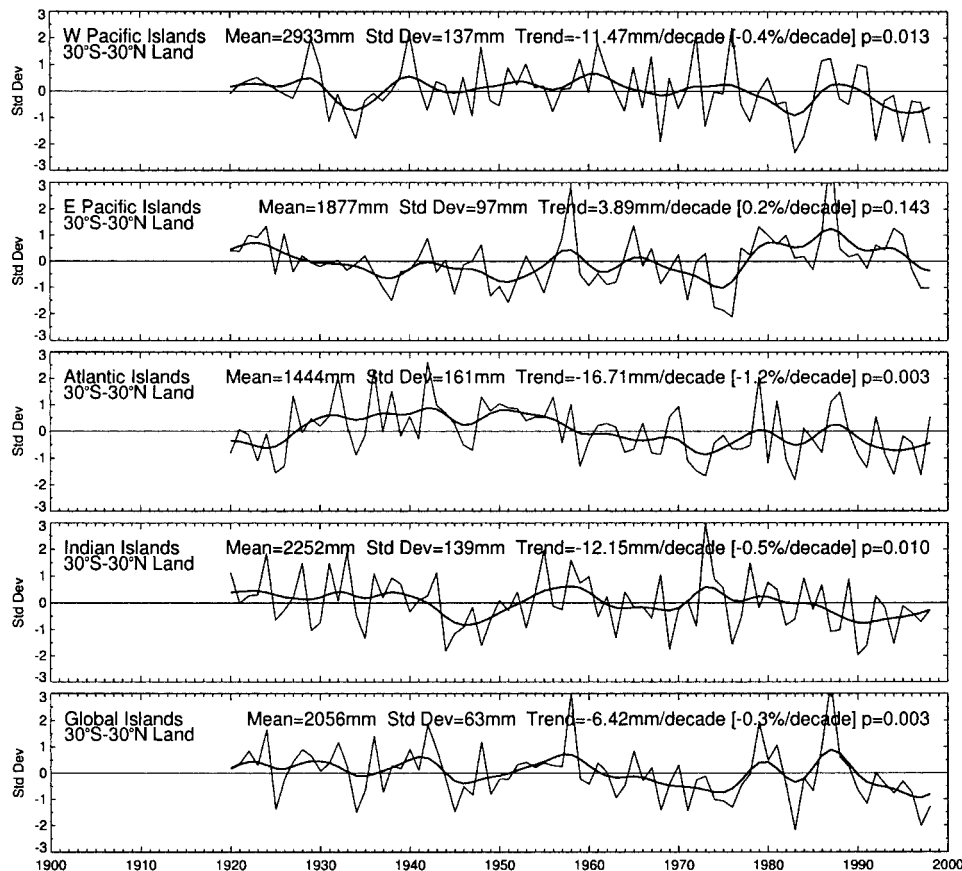
Figure 4. Trends in annual precipitation over the oceans between 30°S and 30°N. Series are derived from 'land' cells in the gauge-based NEW dataset (regridded to 2.5° latitude/longitude resolution), of which there were 130, 23 and 17 cells in the Pacific, Indian and Atlantic domains respectively

Of these, the latter is perhaps of greatest significance in the context of trend detection. A number of studies have sought to correct for this bias. Chu and Wang (1997) analysed a bias-corrected OLR dataset spanning the period 1974–1992 in which a decrease (increase) in OLR over the tropical central-western Pacific and Indian Ocean (northern Australia) was identified, suggested an increasing (decreasing) trend in deep convective precipitation. Seasonal analysis suggested an intensification of the Asian summer monsoon. In the Southern Hemisphere an increase in summer convection was apparent over the equatorial south-central Pacific and the south-central Indian Ocean. Even after removal of El Niño and La Niña years, the trends remained in many regions suggesting that monsoon convection over the western Pacific and Indian Ocean has undergone a change in mean climate state, possibly on a decadal time-scale.

Waliser and Zhou (1997) used Rotated Empirical Orthogonal Function (REOF) analysis to distinguish between natural and artificial (associated with (iv) above) modes of variability in the OLR and Highly Reflective Cloud (HRC) datasets. Bias correction was attempted by modifying the time series of the REOFs associated with artificial modes (using information on satellite orbital characteristics) and removing this from the original data. Both the corrected HRC and OLR datasets indicate a significant increase in convection over the tropical western Pacific.

Information on trends in extratropical regions using these data is precluded by the weak link between OLR from cloud tops and surface precipitation. Tait et al. (1999) describe the development of a satellite microwave precipitation climatology for the northeast Atlantic region from which it was demonstrated that precipitation correlated strongly with recognized modes of climate variability in the region.

Satellite data have also proved useful in monitoring precise trends in atmospheric moisture. Wentz and Schabel (2000) analysed 11 years of atmospheric water vapour estimates over the global oceans between 60°N and 60°S, derived from SSM/I data. A positive trend of 1–2% per decade, depending on latitude, was identified in association with similar trends in surface and tropospheric temperatures. The results are thus consistent with a constant relative humidity model for the atmosphere.

The longest record of monthly precipitation that includes the oceans is the CMAP dataset (Xie and Arkin, 1996; see Section 4), which extends from 1979 to present. Although relatively short, the CMAP data permit an analysis of decadal and interannual variability over the last two decades (Plate 2). Precipitation has a decreasing trend over much of the ocean between 10° and 30°S, with the exception of the eastern (drier regions) boundaries of the Pacific and Atlantic oceans, where precipitation has increased. A similar but less pronounced pattern is evident in the northern tropical oceans. These decreases are contrasted by increased precipitation between 5°S and 5°N over most of Pacific and the Atlantic, and alternate bands of increased-decreased-increased precipitation over 30°–45°S, 45°–60°S and 60°–75°S. These trends remain essentially unchanged when the effects of ENSO variability are removed from the dataset (i.e. there is no trend in ENSO between 1979 and 1999), suggesting that there may be a shift in the zonal distribution of precipitation. However, the short time period of analysis means that these 'trends' may simply represent decadal-scale variability rather than secular change.

5.4. Modes of variability

Precipitation over land in the tropics has been shown by many authors to be dominated by an ENSO signal. This is confirmed in Table V, which shows the marked correlations between the Southern Oscillation Index (SOI; as defined by Ropelewski and Jones, 1987; Konnen *et al.*, 1998) and annual zonal precipitation in the both the northern tropics ($r = 0.62$) and southern tropics ($r = 0.59$). The reasons for this can be seen in Plate 3, which shows the correlations between annual precipitation at individual grid points (NEW dataset regridded to 2.5° latitude/longitude) and the annual SOI for the period 1901–1998. Positive correlations—below normal precipitation in El Niño years where the pressure at Darwin is high compared with Tahiti—predominate over land in the tropics, both annually and in most seasons, and combine to produce the positive correlations seen in the zonal averages. In contrast, in the southern subtropics, positive correlations over Australia and Southern Africa are countered by negative correlations over South America and the resulting (positive) correlation with zonal precipitation is only 0.21. There are also areas of marked negative correlation between SOI and zonal precipitation in the northern subtropics and temperate zones (Table V). Spatially, these correlations are strongest over North America and Central Asia. Stronger correlations in some regions can be obtained from a lagged relationship with SOI (not shown, but c.f. Ropelewski and Halpert, 1996) but do not markedly alter the patterns in Plate 3.

Table V. Correlations between indices of atmospheric pressure oscillation and precipitation (annual and seasonal) over various domains

	Global	NH	SH	60°–80°N	40°–60°N	20°–40°N	0°–20°N	0°–20°S	20°–40°S	40°–60°S
SOI Ann	0.62	0.39	0.59	−0.05	−0.33	−0.28	0.62	0.59	0.21	0.03
NAO Ann	−0.13	−0.13	−0.07	0.07	−0.27	0.16	−0.11	−0.08	0.01	−0.03
NAO DJF	−0.18	−0.04	−0.20	0.25	−0.29	0.16	−0.05	−0.17	−0.10	−0.12
AO Ann	−0.03	−0.09	0.02	0.51	−0.33	0.23	−0.18	−0.01	0.13	−0.18
AO DJF	−0.14	−0.13	−0.09	0.69	−0.59	0.14	−0.10	−0.15	0.10	−0.14
AAO Ann	0.07	0.06	0.04	0.21	0.10	0.28	−0.13	0.01	0.13	−0.06
AAO DJF	0.25	0.03	0.31	0.09	0.09	−0.16	0.06	0.30	0.18	−0.38
AAO JJA	−0.08	−0.14	0.03	0.04	−0.01	0.26	−0.27	0.05	0.06	−0.30

SOI and NAO are from the Climatic Research Unit (CRU, 2000), the AO and AAO are calculated from NCEP reanalysis SLP fields (after Thompson *et al.*, 2000) and the precipitation series are as for Figure 3.
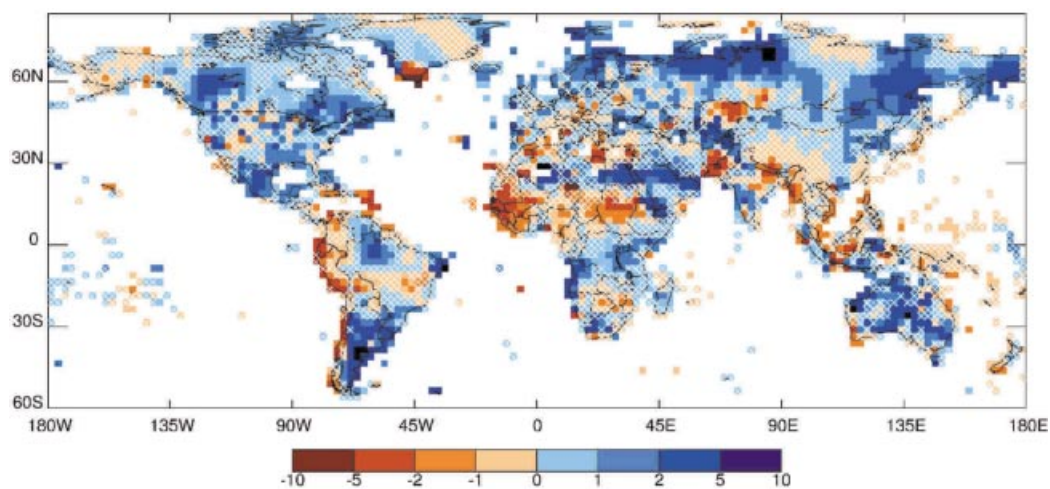
Plate 1. Spatial patterns of trends in annual precipitation from 1901 to 1998 in the dataset of New *et al*. (2000). Trends are expressed as percentages (per decade) of the 1901–1998 mean; trends with a *greater* than 10% ($p = 0.10$) probability of arising from a random series (see Figure 3) are hatched
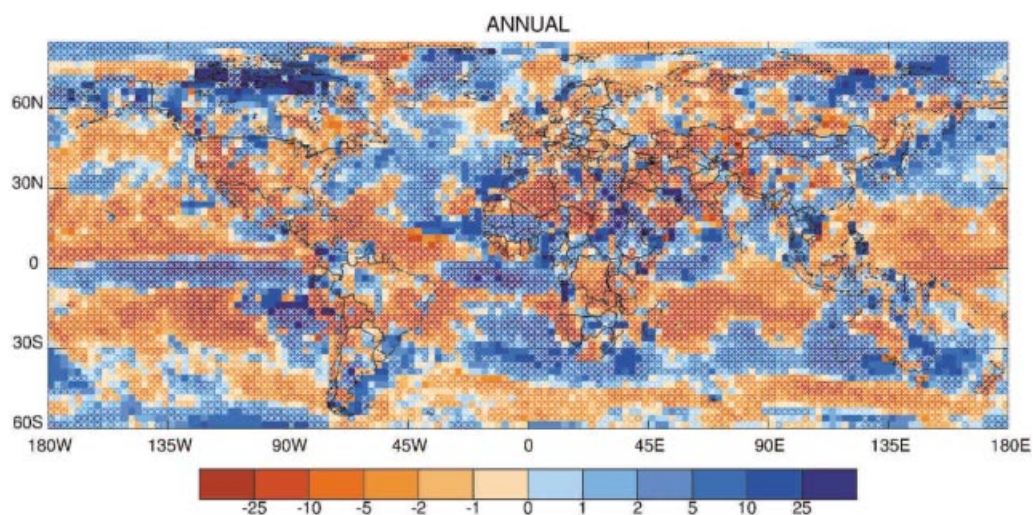

Plate 2. Spatial patterns of trends in annual precipitation from 1979–1999 in the CMAP dataset (Xie and Arkin, 1996a). Trends are expressed as percentages (per decade) of the 1979–1999 mean and those with a *greater* than 10% ($p = 0.10$) probability of arising from a random series (see Figure 3) are hatched
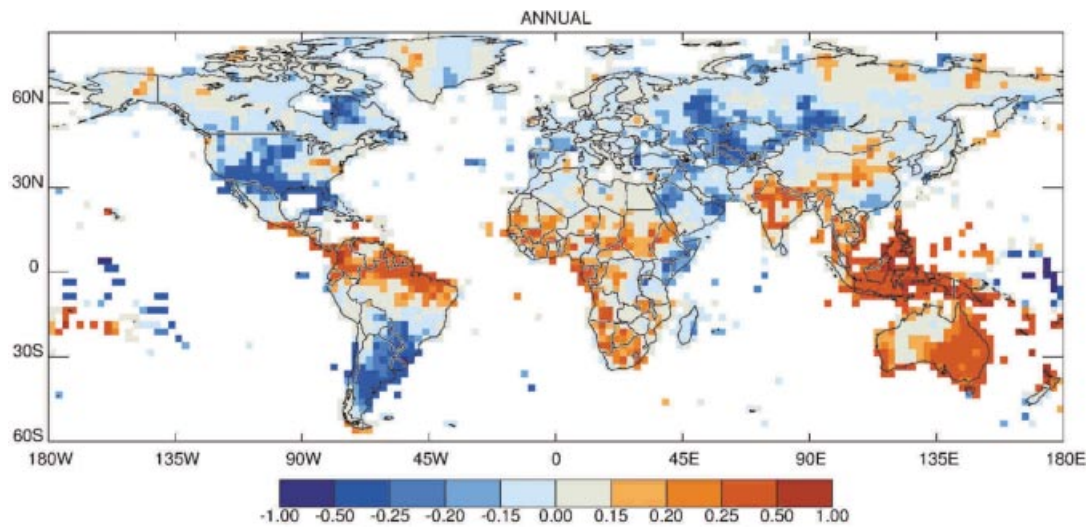
Plate 3. Grid-point correlations between SOI and annual precipitation over land in the gauge-based NEW dataset (1901–1998). Correlations of ±0.15, ±0.20 and ±0.25 correspond roughly to 10%, 5% and 1% significance levels (for a sample size of 100)
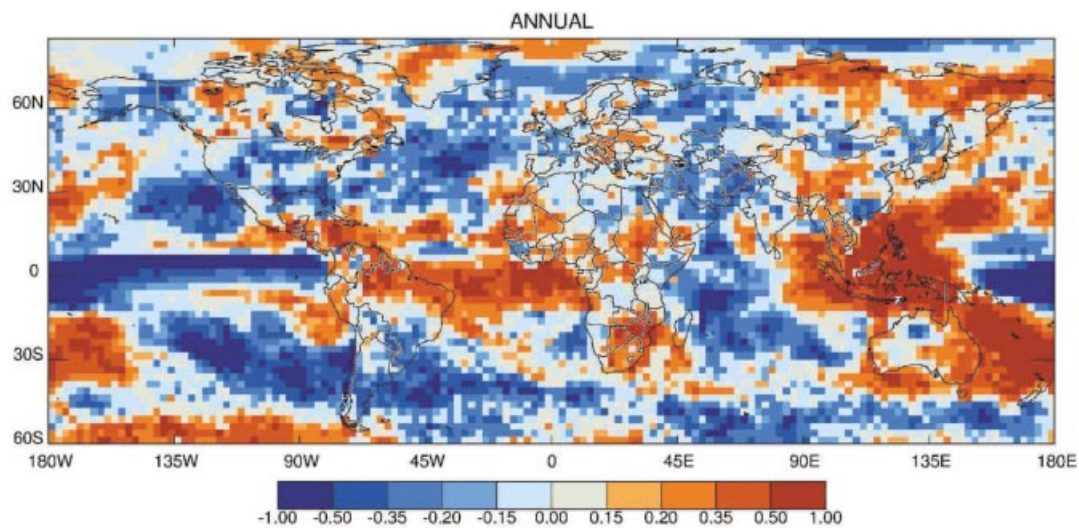

Plate 4. Grid-point correlations between SOI and annual precipitation over land and ocean in the CMAP dataset (1979–1999). Correlations of ±0.35, ±0.42 and ±0.50 correspond roughly to 10%, 5% and 1% significance levels (for a sample size of 20)

The above patterns agree with analyses by others (Ropelewski and Halpert, 1986, 1996; Dai et al., 1997). Using EOF analyses, Dai et al. (1997) found that the leading EOF, representing 6.3% of the total variance of global land precipitation, replicates the ENSO sea surface temperature cycles in the tropical Pacific (correlation of 0.89). The strength of the ENSO signal is seasonally dependent and is usually strongest during the rainy season(s) in any region. For example, the North American centre of activity moves from 40°–50°N in winter and summer to 25°–40°N in autumn and spring (probably a function of where precipitation is occurring), while the correlations over East Africa are strongest in spring and autumn.

The CMAP precipitation dataset permits an analysis of ENSO variability over land and ocean over the last 20 years (e.g. Dai and Wigley, 2000). Plate 4 shows the correlation between the SOI and annual precipitation at each 2.5° grid point in the CMAP dataset. The correlations with SOI seen over land for the period 1901–1998 (Plate 3) are replicated over the shorter period but are now also visible over ocean areas. In the tropics the correlations represent eastward shifts in the major centres of tropical convection over the Pacific, Atlantic (and Amazonia) and Africa/Indian Ocean associated with El Niño and La Niña. Also apparent are correlations related to shifts in the associated subtropical convergence zones, extending southeast and northeast away from the equatorial zone (also identified by Dai and Wigley, 2000), confirming the ENSO tropical-temperate linkages identified in other studies (e.g. Jury, 1992; Vincent, 1994). The main locus of this extension is the Pacific, where positive correlations over Indonesia (dry during El Niño) extend both northeast and southeast to about 45°N/S (representing shifts in the South Pacific Convergence Zone or SPCZ, and the Baiu frontal zone, a northern summer equivalent of the SPCZ). These 'arms' are separated in the central Pacific by negative correlations (wetter during El Niño), which also propagate southeast and northeast, crossing South and North America and extending into the Atlantic Ocean. This pattern is repeated, but less distinctly, over the South Atlantic and the Southern Africa-Indian Ocean Convergence Zones. The mean position of the SPCZ, SACZ and the African cloud bands lie in the zones of zero correlations between the east/west correlation dipoles. There are also similar, but weaker correlations extending to the northeast over the Atlantic and Africa-Indian Ocean domains.

The North Atlantic Oscillation (NAO) is an important mode of atmospheric variability over the North America–Atlantic–Europe region, accounting for about 10% of the variance in land precipitation over this domain (Dai et al., 1997). A high NAO index—the difference between normalized pressures between the Azores (or Portugal) and Iceland (Hurrell, 1995; Jones et al., 1997)—is associated with anomalously high pressure over the north Atlantic, above normal precipitation over northern Europe and southeast North America, and reduced precipitation over southern Europe and north eastern North America. These relationships are stronger in the Northern Hemisphere winter than summer (Hurrell and van Loon, 1997), particularly for high-latitude precipitation (see Table V). The NAO tends to exhibit variability on 1–2 and 7–11 year time scales, but has not exhibited a marked trend over the twentieth century.

The leading modes of interannual variability in the global extratropical circulation are the Antarctic Oscillation (AAO) and Arctic Oscillation (AO; Thompson and Wallace, 2000). These phenomena are characterized by deep, zonally symmetric structures with pressure anomalies of opposite sign in the polar cap regions and a zonal ring near 45°N/S. An AO (AAO) index is defined by the standardized leading principal component time series of monthly mean surface level pressure (850 hPa geopotential height) fields polewards of 20°N (20°S) derived from the NCEP reanalysis dataset (Thompson et al., 2000). The NAO and AO are highly correlated (0.79 in DJF, 0.57 for annual average) and there is some debate about the extent to which the NAO is simply a regional manifestation of the AO. The AO is highly correlated with land precipitation in mid- and high latitudes, especially in winter ($r = 0.69$ for DJF 60°–80°N precipitation and $r = -0.59$ for annual 40°–60°N precipitation); this is about double the corresponding correlations with the NAO (Table V), supporting the suggestion that the AO is the dominant mode of variability in the northern extratropics. The AAO appears to be a less important influence on southern hemisphere precipitation (maximum correlation is -0.38 for DJF precipitation at 40°–60°S), but it should be noted that high latitude land precipitation incorporates only southern South America, New Zealand and Tasmania, and so is rather unrepresentative of the average zonal precipitation. Correlations

between the AAO and complete zonal averages calculated from the XIE dataset are higher (up to 0.51) but the XIE dataset is relatively short and subject to considerable uncertainty at these latitudes. The AO and AAO both exhibit increasing trends over the last 40 years, particularly in their respective winter seasons (see Thompson *et al.*, 2000 for a comprehensive discussion). These trends may be related to the zonal trends in precipitation over the last 20 years (see Section 5.3) and the observed polewards shift of the southern hemisphere subtropical wind maximum (Gibson, 1992).

5.5. Changes in precipitation intensity and duration

Changes in the character of precipitation may occur with or without changes in total precipitation. For example, there may be a shift towards fewer but more intense precipitation events in a season or year (i.e. the distribution of precipitation events), without a change in the total amount of precipitation. However, a more general case involves concurrent changes in both the distribution of precipitation events and in total precipitation depth. Analysis of such changes requires long-term, good quality daily data, which are not available for many regions of the world. Consequently, studies of change in daily precipitation and its structure have tended to be country-specific or regional in extent. Although regional variations are apparent, many studies have identified an increase in the 'intensity' of daily precipitation over the twentieth century. Most studies have differing definitions of intense precipitation, which makes comparison of results problematic (e.g. Haylock and Nicholls, in press). The following represents a summary of recent results.

Karl and Knight (1998) analysed daily precipitation data from the USA for the period 1910–1996. They found a ∼10% increase in annual precipitation, with over half this trend being caused by increases in the upper 10th percentile of daily precipitation. Most of the increases were due to a greater number of rain days (about 6.3 days/century), with the greatest contribution arising from an increase in the number of heavy/extreme precipitation events.

Statistical analyses of daily precipitation over Canada, the USA, Mexico, the former Soviet Union, China, Australia, Norway, and Poland (Groisman *et al.*, 1999), which represent about 40% of global land areas, showed increases in summer precipitation (except for China) of about 5% over the past century. Over Australia, twentieth century annual total precipitation exhibits an increasing trend of 14–18% over much of the continent (Hennessy *et al.*, 1999). The regional pattern of changes in the distribution of daily precipitation was less distinct with both increases in and decreases in heavy and light precipitation, but over Australia as a whole, the number of rain days has increased by 10% (Hennessy *et al.*, 1999; Haylock and Nicholls, 2001).

Over South Africa, Mason *et al.* (1999) have shown that between 1931–1960 and 1961–1990 increases in extreme precipitation have occurred over ∼70% of the country, and that these increases were greatest for the most extreme events. Similarly, for Japan, Iwashima and Yamamoto (1993) analysed daily precipitation and found that more stations recorded their highest, second highest or third highest precipitation event in the most recent decades.

Osborn *et al.* (2000) analysed heavy precipitation events (defined as daily precipitation contributing at least 10% of the seasonal precipitation total) at 110 stations over the UK for the 1961–1995 period. The analysis method was similar to Karl and Knight (1998) but the thresholds used, which vary from station to station, were determined by precipitation amount rather than by frequency. In winter (summer) there has been an increase (decrease) in the contribution of these heavy events to seasonal totals. In spring and autumn no changes were evident.

These regional analyses provide evidence for widespread increases in the intensity of daily precipitation. Analyses of monthly precipitation provide additional information on the persistence of extreme events (e.g. Dai *et al.*, 1997). Plate 5 shows the fractional increase between the first and second halves of the twentieth century in the number of dry and wet spells of 3 or more months' duration. In this analysis, wet (dry) months are defined as those that are greater (less) than 0.5 standard deviations of the century mean monthly precipitation. Spell frequencies were calculated using monthly data in the GHCN/HULME station datasets, and then gridded to 2° latitude/longitude resolution by calculating a simple average of all

0.5-Sigma Above Average
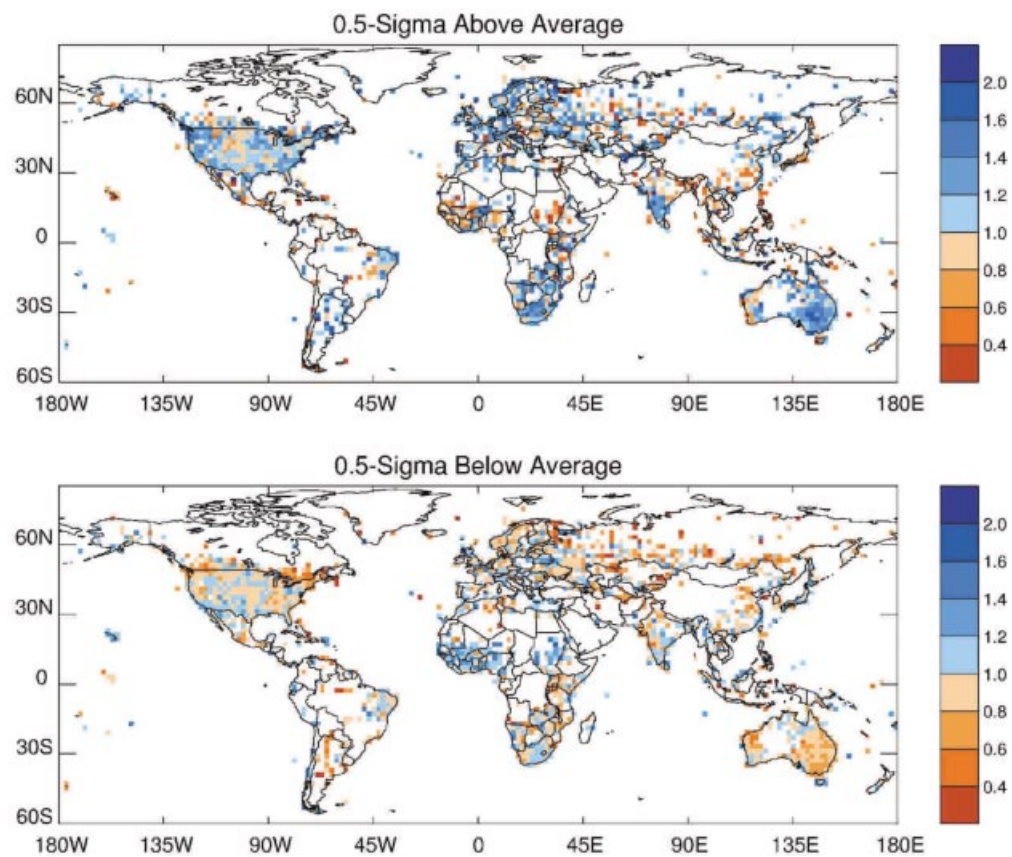

0.5-Sigma Below Average

Plate 5. Change in the frequency of occurrence of wet and dry spells of 3-month duration between 1901–1950 and 1951–1998. Scale units are the ratio of the number of spells in the period 1951–1998 to those in the period 1901–1950 (see text for more detail)

contributing stations in each 2° grid cell. Stations were required to have at least 25 years of data in each period for inclusion; because of this requirement there are large portions of global land areas with no coverage.

As might be expected from the overall increase in global precipitation (Section 5.1), there is a general increase in the frequency of wet spells. Areas with relatively coherent increases in the frequency of wet spells include the USA and Canada, Europe, southern Africa and Australia. Although station data are sparse, there is evidence that wet spell frequency has also increased at high northern latitudes, but at least a proportion of this is likely to arise from the instrumental biases described earlier. A reduction in the frequency of wet spells has occurred over the mid-western USA, tropical North Africa, the western seaboard of Australia and over the Asian monsoon region. These results agree qualitatively with the analyses of daily precipitation described earlier, suggesting that over much of the global land area, there has been an increase in the intensity of precipitation events on daily to tri-monthly time scales.

In most regions where the frequency of wet spells has increased, there has been a corresponding decrease in the frequency of dry spells. However, there are a few regions where there is a suggestion that the change in frequency of wet and dry spells have the same sign. Over central South Africa and Southeast India there is an increased frequency of both wet and dry spells, indicating that the precipitation climate has become noticeably more variable in the second half of the century. In contrast, there is a tendency for decreased frequency of both wet and dry spells over central Asia, suggesting a decrease in the variability of monthly precipitation over these regions.

6. DISCUSSIONS AND CONCLUSIONS

Long-term records are essential for monitoring secular trends and multi-decadal variability in precipitation. There are two main sources of precipitation data, surface rain gauge measurements and satellite estimates. The former remain the ultimate ground-truth for satellite estimates and provide coverage over (most) global land areas through the twentieth century. However, they provide sparse coverage over oceanic areas, where gauge measurements are restricted to oceanic islands, and in many cold and arid regions. Consequently, precipitation gauge records extending from early in the twentieth century represent only about 25% of the Earth's surface, and relatively little of the tropics, where the bulk of world precipitation occurs. In contrast, satellite estimates provide (potentially) spatially complete coverage at a range of space–time scales that are sensor- and platform-dependent. The main disadvantages of using satellite estimates for analysis of long-term precipitation variability and trends are the relatively short records (maximum ∼ 20 years) and discontinuities arising from platform/sensor changes and orbital variations.

Gauge records are also subject to inhomogeneities, mainly due to instrument and location changes. Such inhomogeneities are rarely systematic over an entire region: those not large enough to be detected will tend to cancel each other out when used in regional analyses. The exception to this is where instrumental changes or changes in measurement practice occur over an entire country, such as the change to gauges with more efficient snow catch that occurred in the former USSR in the 1950s. Most national datasets of monthly precipitation gauge data have undergone extensive data quality control and inhomogeneity adjustment and are thought to be relatively unbiased. Care needs to be exercised with global datasets, however, which may not always reflect these national adjustments.

Precipitation gauge measurements indicate that global land precipitation (excluding Antarctica) has increased by about 9 mm over the twentieth century (a trend of 0.89 mm/decade). This trend is small relative to interannual and interdecadal variability. When viewed spatially, the trends in annual precipitation are positive over most land areas, apart from tropical North Africa, which contributes a 0.14 mm/decade decreasing trend to the global precipitation time series. Other regions with coherent decreasing trends are Botswana/Zimbabwe, parts of the Amazon basin and western South America. Within the century-long trend, global precipitation exhibits considerable variability on decadal time scales, up to ± 40 mm. Zonally averaged precipitation exhibits marked increasing trends between 40°–60°N and

60°–80°N and a marked decreasing trend of 0.10 mm/decade over 0°–20°N (the tropical North African influence) and 20°–40°S. Precipitation trends in other zones are not as marked when compared with interannual variability of the series.

The dominant mode of variability in global and hemispheric land precipitation is related to ENSO, which explains about 38% of the interannual variance in globally averaged land precipitation (35% and 15% of Southern Hemisphere and Northern Hemisphere precipitation respectively) and about 8% of the space–time variability of global precipitation. The ENSO signal is strongest in the tropics, which in turn dominates global precipitation variability. In the extratropics, ENSO has a strong influence over the southern and Midwest USA, South America and parts of central Asia. In the mid- and high latitudes the AO and AAO are the dominant modes of interannual climate variability. The AO explains 48% and 35% of winter precipitation variability over land in the latitude bands 60°–80°N and 40°–60°N, respectively. The AAO appears less important, although precipitation data from high latitudes in the Southern Hemisphere are sparse. The NAO is not an important modulator of global precipitation, but it does explain 8% of annual variability in spatially averaged Northern Hemisphere mid-latitude precipitation. The NAO has a stronger influence on winter precipitation at northern mid- and high latitudes.

Analyses of precipitation over land and ocean (spatially complete) since 1980 indicate only a few regions have marked trends in precipitation over this short period. However, there is a suggestion that there has been a zonal shift in precipitation, with increases around the equator and at 30°–40°N/S, and decreases between 10°–20°N/S and 40°–60°N/S. As with land precipitation over the twentieth century, ENSO is correlated with oceanic precipitation over much of the tropics. The inclusion of 20 years of ocean precipitation in the analysis enabled the identification regions where the tropical ENSO signal extends in a northeast/southeast direction into the subtropics. These extensions are strongest over the Pacific–Indonesian region, but are also present over the Atlantic–African and Indian Ocean domains and are associated with variability in the tropical-temperate cloud bands.

There is evidence from North America, Europe, southern Africa, Japan and Australia of increasing intensity in daily precipitation, particularly during summer. These intensity changes have often manifested themselves through increased frequency of wet days and an increased proportion of total precipitation occurring during the heaviest events. Over most land areas there has been an increase in the persistence of wet spells (periods with 3 or more consecutive months with precipitation more than one standard deviation greater than the twentieth century mean). Over tropical North Africa, the frequency of wet spells has decreased because of the post-1965 Sahelian drought. In most regions increased (decreased) wet spell frequency is mirrored by decreased (increased) dry spell frequency. Notable exceptions are central South Africa and Southeast India, where there is an increased frequency of wet *and* dry spells, suggesting that monthly precipitation has become more variable, and central Asia where the occurrence of wet and dry spells have both decreased (suggesting a decrease in the variability of monthly precipitation).

In contrast to the global temperature record (Jones *et al.*, 1999), it is difficult to argue that there has been a significant trend (in either a qualitative or a statistical sense—see Nicholls (2001) for a discussion of the problems with significance testing in atmospheric science) in global land precipitation through the twentieth century. The reduction in precipitation over North Africa has counteracted the increasing trend over most other land areas. This may be a real geographically significant climate change signal, in which case global land precipitation has not changed markedly. Conversely, if the North African drying is independent of the background trend in global precipitation then a reversal to pre-1965 conditions over this region may result in the evolution of a marked upward trend in global precipitation. A second problem in the analysis of twentieth century precipitation lies in the absence of data from the oceans prior to 1980, so there is no information about the behaviour of precipitation over about 60% of the globe prior to the late 1970s. Area-averaged estimates of precipitation over tropical oceanic islands show an overall decreasing trend in tropical oceanic precipitation during the twentieth century. This suggests that there may have been a decrease in precipitation over the tropical oceans, which counterbalances the increase over land. However, these ocean island series are not representative of the tropical (or global) oceans as a whole and should be treated with caution.

Simulations of twenty-first century climate by general circulation models (GCMs) forced with increasing atmospheric concentrations of greenhouse gases indicate an increase in the intensity of the hydrological cycle as global temperature increases (Kattenberg *et al.*, 1996), manifest as an increase in total precipitation, and increased intensity (more wet days and more heavy precipitation). In the face of these simulations it remains crucially important to improve and maintain existing precipitation gauge datasets to enable more rigorous analyses of global and regional precipitation trends and variability. For gauge-based datasets, this can be achieved through the retrieval (and digitizing) of gauge records from early years (e.g. the Colonial Era Archive Project, NCDC, 1998) and the maintenance of the current network, through the programs such as the Global Climate Observing System (GCOS; Spence and Townshend, 1995; Nowlin *et al.*, 1996; Peterson *et al.*, 1997). GCOS has selected a near 1000 station network for its GCOS Surface Network (GSN). The network was chosen principally for temperature, but precipitation and pressure data are also reported. As this review has shown, 1000 stations are inadequate to monitor regional-scale precipitation trends and variability, but the GSN has been chosen with the specific aim to monitor global trends and large-scale variability. Each country with stations in the GSN has been requested to supply historic data in daily form. When these data are available they will enable more comprehensive studies of changes in the character of daily precipitation.

Satellite-derived estimates of precipitation (and particularly merged multi-satellite/gauge products) clearly provide the greatest potential for precipitation monitoring in the twenty first century. Presently, satellite and merged products support a wide range of studies in regional and global climate variability at interannual and intraseasonal time scales. As we move through the first few decades of this new century, there will be the potential for the development of spatially complete multi-decadal precipitation datasets. In this context the issues raised in Section 5.3 are paramount: there is a clear need to resolve (or at least minimize) problems associated with platform changes and instrument changes/biases that currently restrict the use of satellite products for trend detection. The success of TRMM has prompted plans for a follow-on Global Precipitation Mission which may consist of a constellation of polar orbiting passive microwave sensors (similar to SSM/I) and a single active microwave precipitation radar used largely for calibration of the passive MW algorithms. The aim is to produce truly global estimates of instantaneous rain rate with high spatial and temporal resolution. Nevertheless, whatever successes new satellite technologies may offer, the need for well-maintained and continuous gauge-based precipitation measurements will remain.

REFERENCES

Arkin PA, Meisner BN. 1987. The relationship between large-scale convective rainfall and cold cloud over the western hemisphere during 1982–84. *Monthly Weather Review* **115**: 51–74.

Barrett EC, Adler RF, Arpe K, Bauer P, Berg W, Chang A, Ferraro R, Ferriday J, Goodman S, Hong Y, Janowiak J, Kidd C, Kniveton D, Morrissey M, Olsen W, Petty G, Rudolf B, Shibata A, Smith E, Spencer R. 1994. The first WetNet Precipitation Intercomparison Project (PIP-1): interpretation of results. *Remote Sensing Review* **11**: 303–373.

Bell TL, Kundu PK. 2000. Dependence of satellite sampling error on monthly averaged rain rates: comparison of simple models and recent studies. *Journal of Climate* **13**: 449–462.

Bradley RS, Diaz HF, Eischeid JK, Jones PD, Kelly PM, Goodess CM. 1987. Precipitation fluctuations over Northern Hemisphere land areas since the mid-19th century. *Science* **237**: 171–175.

Chahine MT. 1992. The hydrological cycle and its influence on climate. *Nature* **359**: 373–379.

Chu PS, Wang JB. 1997. Recent climate change in the tropical western Pacific and Indian Ocean regions as detected by outgoing longwave radiation records. *Journal of Climate* **10**: 636–646.

Cramer W, Fischer A. 1996. Data requirements for global terrestrial ecosystem modelling. In *Global Change and Terrestrial Ecosystems*, Walker B, Steffen W (eds). Cambridge University Press: Cambridge; 530–565.

CRU. 2000. Climatic Research Unit data download web pages: http://www.cru.uea.ac.uk/cru/data.

Dai A, Fung I, Del Genio A. 1997. Surface observed global land precipitation variations during 1900–1988. *Journal of Climate* **11**: 2943–2962.

Dai AG, Wigley TML. 2000. Global patterns of ENSO-induced precipitation. *Geophysics Research Letters* **27**: 1283–1286.

Daly R. 1991. *Atmospheric Data Analysis*. Cambridge University Press: Cambridge.

Diaz HF, Bradley RS, Eischeid JK. 1989. Precipitation fluctuations over global land areas since the late 1800s. *Journal of Geophysical Research—Atmosphere* **94**: 1195–1210.

Doherty RM, Hulme M, Jones CG. 1999. A gridded reconstruction of land and ocean precipitation for the extended tropics from 1974 to 1994. *International Journal of Climatology* **19**: 119–142.

Easterling DR, Peterson TC. 1995. A new method for detecting undocumented discontinuities in climatological time-series. *International Journal of Climatology* **15**: 369–377.

Easterling DR, Peterson TC, Karl TK. 1996. On the development and use of homogenised climate datasets. *Journal of Climate* **9**: 1429–1434.

Ebert EE, Manton MJ. 1998. Performance of satellite rainfall estimation algorithms during TOGA COARE. *Journal of the Atmospheric Sciences* **55**: 1537–1557.

Ebert EE, Manton MJ, Arkin PA, Allam RJ, Holpin GE, Gruber A. 1996. Results from the GPCP algorithm intercomparison programme. *Bulletin of the American Meteorological Society* **77**: 2875–2887.

Ferraro RR, Weng FZ, Grody NC, Basist A. 1996. An eight-year (1987–1994) time series of rainfall, clouds, water vapor, snow cover, and sea ice derived from SSM/I measurements. *Bulletin of the American Meteorological Society* **77**: 891–905.

Folland CK, Karl TR. 2001. Observed climate variability and change. In *The Scientific Basis of Climate Change*, Houghton JT, Ding Y, Naugher M, van der Linden PJ, Dai X, Maskell K, Johnson CA (eds). Cambridge University Press: Cambridge, UK; 99–181.

Folland CK, Karl TR, Nicholls N, Nyenzi BS, Parker DE, Vinnikov KY. 1992. Observed climate variability and change. In *Climate Change 1992: The Supplementary Report to the IPCC Scientific Assessment*, Houghton JT, Callander BA, Varney SK (eds). Cambridge University Press: Cambridge; 135–170.

Folland CK, Karl TR, Vinnikov KYA. 1990. Observed climate variations and change. In *Climate Change: The IPCC Scientific Assessment*, Houghton JT, Jenkins GJ, Ephraums JJ (eds). Cambridge University Press: Cambridge; 195–238.

Gibson TT. 1992. An observed poleward shift of the southern hemisphere subtropical wind maximum: a greenhouse symptom? *International Journal of Climatology* **12**: 637–640.

Groisman PY, Karl TR, Easterling DR, Knight RW, Jamason PF, Hennessy KJ, Suppiah R, Page CM, Wibig J, Fortuniak K, Razuvaev VN, Douglas A, Forland E, Zhai PM. 1999. Changes in the probability of heavy precipitation: important indicators of climatic change. *Climate Change* **42**: 243–283.

Groisman PY, Koknaeva VV, Belokrylova TA, Karl TR. 1991. Overcoming biases of precipitation measurement: a history of the USSR experience. *Bulletin of the American Meteorological Society* **72**: 1725–1733.

Groisman PY, Legates DR. 1995. Documenting and detecting long-term precipitation trends: where are we and what should be done? *Climate Change* **31**: 601–622.

Groisman PY, Rankova EY. 2001. Precipitation trends over the Russian permafrost-free zone: Removing the artifacts of preprocessing. *International Journal of Climatology* **21**: 657–678.

Gruber A, Krueger AF. 1984. The status of the NOAA outgoing longwave radiation data set. *Bulletin of the American Meteorological Society* **65**: 958–962.

Haylock M, Nicholls N. In press. Trends in extreme rainfall indices for an updated high quality data set for Australia, 1910–1998. *International Journal of Climatology*.

Heino R. 1994. *Climate in Finland During the Period of Meteorological Observations*. Finnish Meteorological Institute: Helsinki.

Hennessy KJ, Suppiah R, Page CM. 1999. Australian rainfall changes, 1910–1995. *Australian Meteorological Magazine* **48**: 1–13.

Hsu KL, Gupta HV, Gao XG, Sorooshian S. 1999. Estimation of physical variables from multichannel remotely sensed imagery using a neural network: application to rainfall estimation. *Water Resources and Research* **35**: 1605–1618.

Huffman GJ, Adler RF, Arkin P, Chang A, Ferraro R, Gruber A, Janowiak J, McNab A, Rudolf B, Schneider U. 1997. The Global Precipitation Climatology Project (GPCP) Combined Precipitation Dataset. *Bulletin of the American Meteorological Society* **78**: 5–20.

Huffman GJ, Adler RF, Morrissey MM, Curtis S, Joyce R, McGavock B, Susskind J. 2000. Global precipitation at 1 degree daily resolution from multi-satellite observations. *Journal of Hydrometeorology* **2**(1): 36–50.

Hulme M. 1994a. Validation of large-scale precipitation fields in General Circulation Models. In *Global Precipitation and Climate Change*, Desbois M, Desalmand F (eds). Springer: Berlin; 387–405.

Hulme M. 1994b. The cost of climate data—a European experience. *Weather* **49**: 168–175.

Hulme M, Barrow EM, Arnell NW, Harrison PA, Johns TC, Downing TE. 1999a. Relative impacts of human-induced climate change and natural climate variability. *Nature* **397**: 688–691.

Hulme M, Mitchell JFB, Jenkins J, Gregory JM, New M, Viner D. 1999b. Global climate scenarios for fast-track impacts studies. *Global and Environmental Change;* Supplementary Issue: S3–S19.

Hurrell JW. 1995. Decadal trends in the North Atlantic Oscillation—regional temperatures and precipitation. *Science* **269**: 676–679.

Hurrell JW, van Loon H. 1997. Decadal variations in climate associated with the north Atlantic oscillation. *Climate Change* **36**: 301–326.

IPCC. 1996. *Climate Change 1995: The Science of Climate Change*. Cambridge University Press: Cambridge.

Iwashima T, Yamamoto R. 1993. A statistical analysis of extreme events: long-term trend of heavy daily precipitation. *Journal of the Meteorological Society of Japan* **71**: 637–640.

Jones PD, Briffa KR, Osborn TJ, Moberg A, Bergstrom H. In press. Relationships between circulation strength and the variability of growing season and cold season climate in Northern and Central Europe. *Holocene*.

Jones PD, Hulme M. 1996. Calculating regional climatic time series for temperature and precipitation: methods and illustrations. *International Journal of Climatology* **16**: 361–377.

Jones PD, Jonsson T, Wheeler D. 1997. Extension to the North Atlantic Oscillation using early instrumental pressure observations from Gibraltar and south-west Iceland. *International Journal of Climatology* **17**: 1433–1450.

Jones PD, New M, Parker DE, Martin S, Rigor IG. 1999. Surface air temperature and its changes over the past 150 years. *Reviews of Geophysics* **37**: 173–199.

Jury MR. 1992. A climatic dipole governing the inter-annual variability of convection over the southwest Indian Ocean and southeast African region. *Trends in Geophysics Research* **1**: 165–172.

Karl TR, Knight RW. 1998. Secular trends of precipitation amount, frequency, and intensity in the United States. *Bulletin of the American Meteorological Society* **79**: 231–241.

Kastellet E, Nesje A, Pedersen ES. 1998. Reconstructing the palaeoclimate of Jaeren, southwestern Norway, for the period 1821–1850, from historical documentary record [full text delivery]. *Geographical Annals Series A—Physical Geography* **80A**: 51–65.

Kattenberg A, Giorgi F, Grassl H, Meehl GA, Mitchell JFB, Stouffer RJ, Tokioka T, Weaver AJ, Wigley TML. 1996. Climate models: projections of future climate. In *Climate Change 1995: The Science of Climate Change*, IPCC CK (ed.). Cambridge University Press: Cambridge; 285–357.

Kidd CK. 2001. Satellite rainfall climatology. *International Journal of Climatology* **21**: 1041–1066.

Konnen GP, Jones PD, Kaltofen MH, Allan RJ. 1998. Pre-1866 extensions of the Southern Oscillation index using early Indonesian and Tahitian meteorological readings. *Journal of Climate* **11**: 2325–2339.

Kummerow C, Giglio L. 1994a. A Passive Microwave Technique for estimating rainfall and vertical structure information from space. 1. Algorithm description. *Journal of Applied Meteorology* **33**: 3–18.

Kummerow C, Giglio L. 1994b. A Passive Microwave Technique for estimating rainfall and vertical structure information from space. 2. Applications to SSM/I data. *Journal of Applied Meteorology* **33**: 19–34.

Kummerow C, Barnes W, Kozu T, Shiue J, Simpson J. 1998. The Tropical Rainfall Measuring Mission (TRMM) sensor package. *Journal of Atmospheric and Ocean Technology* **15**(3): 809–817.

Legates DR, DeLiberty TL. 1993. Precipitation measurement biases in the United States. *Water Resources Bulletin* **29**: 855–861.

Legates DR, Willmott CJ. 1990. Mean seasonal and spatial variability in gauge-corrected, global precipitation. *International Journal of Climatology* **10**: 111–127.

Mason SJ, Waylen PR, Mimmack GM, Rajaratnam B, Harrison JM. 1999. Changes in extreme rainfall events in South Africa. *Climate Change* **41**: 249–257.

Middleton WEK. 1953. *Meteorological Instruments.* University of Toronto Press: Toronto.

Middleton WEK. 1965. *A History of the Theories of Rain: And Other Forms of Precipitation.* Oldbourne: London.

NCDC. 1998. The colonial era archive data project: historical data for data sparse underdeveloped countries. Available on-line from http://www.ncdc.noaa.gov/ol/climate/research/ghcn/colonialarchive.html.

New M. 1999. Uncertainties in observed climate. In *Representing Uncertainty in Climate Change Scenarios and Impact Studies*, Carter T, Hulme M, Viner D (eds). Climatic Research Unit: Norwich; 59–66.

New M, Hulme M, Jones P. 1999. Representing twentieth-century space-time climate variability. Part I: development of a 1961–90 mean monthly terrestrial climatology. *Journal of Climate* **12**: 829–856.

New MG, Hulme M, Jones PD. 2000. Representing twentieth-century space-time climate variability. Part II: development of 1901–1996 monthly grids of terrestrial surface climate. *Journal of Climate* **13**: 2217–2238.

Nicholls N, Gruza GV, Jouzel J, Karl TR, Ogallo LA, Parker DE. 1996. Observed climate variability and change. In *Climate Change 1995: The Science of Climate Change*, IPCC (ed.). Cambridge University Press: Cambridge; 133–192.

Nicholls N. 2001. The insignificance of significance testing. *Bulletin of the American Meteorological Society* **82**: 981–986.

Nowlin WD, Smith N, Needler G, Taylor PK, Weller R, Schmitt R, Merlivat L, Vezina A, Alexiou A, McPhaden M, Wakatsuchi M. 1996. An ocean observing system for climate. *Bulletin of the American Meteorological Society* **77**: 2243–2273.

Ohara SL, Metcalfe SE. 1995. Reconstructing the climate of Mexico from historical records. *Holocene* **5**: 485–490.

Osborn TJ, Hulme M, Jones PD, Basnett TA. 2000. Observed trends in the daily intensity of United Kingdom precipitation. *International Journal of Climatology* **20**: 347–364.

Peterson T, Daan H, Jones P. 1997. Initial selection of a GCOS surface network. *Bulletin of the American Meteorological Society* **78**: 2145–2152.

Peterson TC, Easterling DR, Karl TR, Groisman P, Nicholls N, Plummer N, Torok S, Auer I, Boehm R, Gullett D, Vincent L, Heino R, Tuomenvirta H, Mestre O, Szentimrey T, Salinger J, Forland EJ, Hanssen-Bauer I, Alexandersson H, Jones P, Parker D. 1998. Homogeneity adjustments of in situ atmospheric climate data: a review. *International Journal of Climatology* **18**: 1493–1517.

Peterson TC, Griffiths JF. 1997. Historical African data. *Bulletin of the American Meteorological Society* **78**: 2869–2872.

Peterson TC, Vose RS. 1997. An overview of the global historical climatology network temperature database. *Bulletin of the American Meteorological Society* **78**: 2837–2849.

Petty GW. 1997. An intercomparison of oceanic precipitation frequencies from 10 special sensor microwave/imager rain rate algorithms and shipboard present weather reports. *Journal of Geophysics Research—Atmosphere* **102**: 1757–1777.

Pfister C, Brazdil R, Glaser R, Barriendos M, Camuffo D, Deutsch M, Dobrovolny P, Enzi S, Guidoboni E, Kotyza O, Militzer S, Racz L, Rodrigo FS. 1999. Documentary evidence on climate in sixteenth-century Europe. *Climate Change* **43**: 55–110.

Piper SC, Stewart EF. 1996. A gridded global data set of daily temperature and precipitation for terrestrial biosphere modeling. *Global Biogeochemistry Cycles* **10**: 757–782.

Rodrigo FS, EstebanParra MJ, PozoVazquez D, CastroDiez Y. 1999. A 500-year precipitation record in Southern Spain. *International Journal of Climatology* **19**: 1233–1253.

Rodrigo FS, Parra MJE, Diez YC. 1995. Reconstruction of total annual rainfall in Andalusia (Southern Spain) during the 16th and 17th centuries from documentary sources. *Theoretical and Applied Climatology* **52**: 207–218.

Ropelewski CF, Halpert MS. 1986. North-American precipitation and temperature patterns associated with the El Niño Southern Oscillation (ENSO). *Monthly Weather Review* **114**: 2352–2362.

Ropelewski CF, Halpert MS. 1996. Quantifying Southern Oscillation—Precipitation relationships. *Journal of Climate* **9**: 1043–1059.

Ropelewski CF, Jones PD. 1987. An extension of the Tahiti–Darwin Southern Oscillation Index. *Monthly Weather Review* **115**: 2161–2165.

Rudolf B, Gruber A, Adler R, Huffman G, Janowiak J, Xie PP. 1999. GPCP precipitation analyses based on observations as a basis for NWP and climate model verification. *Proceedings of WCRP 2nd International Reanalysis Conference*, Reading, UK, 23–27th August, 1999, WCRP-report.

Rudolf B, Hauschild H, Rueth W, Schneider U. 1994. Terrestrial precipitation analysis: operational method and required density of point measurements. In *Global Precipitation and Climate Change*, Desbois M, Desalmand F (eds). Springer: Berlin; 173–186.

Sevruk B. 1982. *Methods of Correction for Systematic Error in Point Precipitation Measurement for Operational Use.* World Meteorological Organisation: Geneva.

Shepard D. 1968. A two-dimensional interpolation function for irregularly spaced data. In *23rd ACM National Conference*. Brabdon Syst. Press: Princeton, USA; 517–524.

Shepard D. 1984. Computer mapping: the SYMAP interpolation algorithm. In *Spatial Statistics and Models*, Gaile GL, Willmott CJ (eds). D Reidel Publishing: Dordrecht; 95–116.

Smith EA, Lamm JE, Adler R, Alishouse J, Aonashi K, Barrett E, Bauer P, Berg W, Chang A, Ferraro R, Ferriday J, Goodman S, Grody N, Kidd C, Kniveton D, Kummerow C, Liu G, Marzano F, Mugnai A, Olson W, Petty G, Shibata A, Spencer R, Wentz F, Wilheit T, Zipser E. 1998. Results of WetNet PIP-2 project. *Journal of the Atmospheric Sciences* **55**: 1483–1536.

Spence T, Townshend J. 1995. The Global Climate Observing System (GCOS). *Climate Change* **31**: 131–134.

Spencer RW. 1993. Global oceanic precipitation from the MSU during 1979–91 and comparisons to other climatologies. *Journal of Climate* **6**: 1301–1326.

Susskind J, Piraino P, Rokke L, Iredell T, Mehta A. 1997. Characteristics of the TOVS Pathfinder Path A dataset. *Bulletin of the American Meteorological Society* **78**: 1449–1472.

Tait AB, Barrett EC, Beaumont MJ, Brown PA, Taberner MJ, Todd MC. 1999. Interpretation of an atlas of passive microwave-derived rainfall over the eastern North Atlantic ocean and North Sea. *International Journal of Climatology* **19**: 231–252.

Thiessen AH. 1911. Precipitation averages for large areas. *Monthly Weather Review* **39**: 1082–1084.

Thompson DWJ, Wallace JM. 2000. Annular modes in the extratropical circulation. Part I: month-to-month variability. *Journal of Climate* **13**: 1000–1016.

Thompson DWJ, Wallace JM, Hegerl GC. 2000. Annular modes in the extratropical circulation. Part II: trends. *Journal of Climate* **13**: 1018–1036.

Todd M, Washington R. 1999. A simple method to retrieve 3-hourly estimates of global tropical and subtropical precipitation from international satellite cloud climatology program (ISCCP) D1 data. *Journal of Atmosphere and Ocean Technologies* **16**: 146–155.

Todd MC, Barrett EC, Beaumont MJ, Bellerby TJ. 1999. Estimation of daily rainfall over the upper Nile river basin using a continuously calibrated satellite infrared technique. *Meteorological Applications* **6**: 201–210.

Todd MC, Barrett EC, Beaumont MJ, Green JL. 1995. Satellite identification of rain days over the upper Nile river basin using an optimum infrared rain no-rain threshold temperature model. *Journal of Applied Meteorology* **34**: 2600–2611.

Todd MC, Kidd CK, Kniveton DR, Bellerby TJ. 2001. A combined microwave and infrared technique for estimation of small scale rainfall. *Journal of Atmosphere and Ocean Technologies* **18**: 742–755.

UNESCO. 1978. *World Water Balance and Water Resources of the Earth.* UNESCO: Leningrad.

Vincent DG. 1994. The South Pacific Convergence Zone (SPCZ): a review. *Monthly Weather Review* **122**: 1949–1970.

Waliser DE, Zhou WF. 1997. Removing satellite equatorial crossing time biases from the OLR and HRC datasets. *Journal of Climate* **10**: 2125–2146.

Wentz FJ, Schabel M. 2000. Precise climate monitoring using complementary satellite data sets. *Nature* **403**: 414–416.

Willmott CJ, Rowe CM, Philpot WD. 1985. Small-scale climate maps: a sensitivity analysis of some common assumptions associated with grid point interpolation and contouring. *American Cartography* **12**: 5–16.

Asdfd WMO. 1996. *Climatological Normals (CLINO) for the Period 1961–1990.* World Meteorological Organisation: Geneva.

Wu MLC. 1991. Global precipitation estimates from satellite-using difference fields of outgoing long-wave-radiation. *Atmosphere-Ocean* **29**: 150–174.

Xie P, Arkin PA. 1996a. Analyses of global monthly precipitation using gauge observations, satellite estimates and numerical model predictions. *Journal of Climate* **9**: 840–858.

Xie P, Arkin PA. 1996b. An intercomparison of gauge observations and satellite estimates of monthly precipitation. *International Journal of Climatology* **34**: 1143–1160.

Xie PP, Rudolf B, Schneider U, Arkin PA. 1996. Gauge-based monthly analysis of global land precipitation from 1971 to 1994. *Journal of Geophysics Research—Atmosphere* **101**: 19023–19034.

Yang D. 1999. An improved precipitation climatology for the Arctic Ocean. *Geophysics Research Letters* **26**: 1625–1628.

Yang DQ, Ishida S, Goodison BE, Gunther T. 1999. Bias correction of daily precipitation measurements for Greenland. *Journal of Geophysics Research—Atmosphere* **104**: 6171–6181.